의학박사학위논문

Investigation of neural mechanisms in neuropathic pain and brain plasticity associated with analgesic effect of transcranial direct current stimulation

신경병증성 통증의 신경학적 기반 및 경두개 직류 전기자극의 진통효과와 관련된 뇌 가소성 연구

2014 년 8 월

서울대학교 대학원

의학과 뇌신경과학 전공

윤 은 진

신경병증성 통증의 신경학적 기반 및 경두개 직류 전기자극의 진통효과와 관련된 뇌 가소성 연구

지도교수 김 상 은

이 논문을 의학박사학위논문으로 제출함
2014 년 7 월

서울대학교 대학원
의학과 뇌신경과학전공
윤 은 진

윤은진의 박사학위논문을 인준함
2014 년 7 월

위 원 장	박 경 석	(인)
부 위 원 장	김 상 은	(인)
위 원	김 지 수	(인)
위 원	이 평 복	(인)
위 원	김 남 희	(인)

Investigation of neural mechanisms in neuropathic pain and brain plasticity associated with analgesic effect of transcranial direct current stimulation

by

Eun Jin Yoon

A Thesis Submitted in Partial Fulfillment of the Requirements for the Degree of Doctor of Philosophy in Medicine (Brain and Neuroscience) at Seoul National University College of Medicine

July 2014

Approved by thesis committee:

Professor	_____	Chairman
Professor	_____	Vice Chairman
Professor	_____	
Professor	_____	
Professor	_____	

Abstract

Investigation of neural mechanisms in neuropathic pain and brain plasticity associated with analgesic effect of transcranial direct current stimulation

Eun Jin Yoon
Graduate Program of Brain and Neuroscience
The Graduate School of Medicine
Seoul National University

Neuropathic pain is one of the major problems of patients with spinal cord injury (SCI), because it remains refractory to treatment despite a variety of therapeutic approach. Therefore, there is the need for development of new therapeutic approaches and understanding the underlying neural mechanisms of neuropathic pain would be a start. Especially, the structural and functional brain study using multimodal imaging tools will give integrative information of the neural mechanisms of neuropathic pain. Recently, it is suggested that transcranial direct current stimulation (tDCS) can produce lasting changes in corticospinal excitability and can potentially be used for the treatment of neuropathic pain. However, the detailed mechanisms underlying the effects of tDCS are unknown.

Sixteen patients suffering from chronic neuropathic pain following SCI (mean age 44.1 ± 8.6 years, 4 females) and 10 healthy controls (39.5 ± 8.6 years, 4 females) underwent [^{18}F]-fluorodeoxyglucose positron emission tomography ([^{18}F]FDG-PET)and magnetic resonance imaging. In study 1, the

structural and functional differences between the patients and healthy controls in brain cortical areas and the structure-function relationships were analyzed. In study 2, the patients received sham or active anodal stimulation of the motor cortex using tDCS for 10 days (20 minutes, 2 mA, twice a day). After the tDCS sessions, [^{18}F]FDG-PET images were acquired from all patients again. The underlying neural mechanisms of tDCS analgesic effect were evaluated by metabolic differences between before and after tDCS. The effect of baseline gray matter volume on brain metabolic changes was also analyzed.

In study 1, we found decreases in gray matter volume in the bilateral dorsolateral prefrontal cortex (DLPFC), and hypometabolism in the medial prefrontal cortex in patients compared to healthy controls. Moreover, the changes in one specific imaging modality were correlated with brain regions composed of default mode network of another modality. In study 2, there was a significant decrease in the numeric rating scale scores for pain, from 7.6 ± 0.5 at baseline to 5.9 ± 1.8 after active tDCS ($z = –2.410$, $p = 0.016$). We found increased metabolism in the stimulation site and the medulla and decreased metabolism in the left DLPFC and precuneus after active tDCS treatment compared with the changes induced by sham tDCS. Additionally, the change in the DLPFC and precuneus was correlated with tDCS efficacy and baseline gray matter volume in these regions.

We found that different imaging modalities commonly identified the possibility of deficits in pain modulation by cognitive and emotional processes in patients with neuropathic pain after SCI and, these abnormal brain changes had correlation with brain regions of default mode network. Moreover the anodal stimulation of the motor cortex using tDCS can modulate these brain regions. Based on these results, we expect that tDCS on

the DLPFC could be effective treatment strategy to patients with neuropathic pain following tDCS.

Keywords: Neuropathic pain, Spinal cord injury, Transcranial direct current stimulation, FDG-PET, MRI, Dorsolateral prefrontal cortex

***Student Number**: 2009-30573*

CONTENTS

List of Tables

List of Figures

Figure 5. To identify the group whose data accounted for the significant differences in treatment effect, brain metabolic changes were analyzed in each group separately. (A) Significant metabolic changes after active tDCS. (B) Significant metabolic changes after sham tDCS. The labels of each slice indicate the *z*-coordinate for axial slices and the *x*-coordinate for the sagittal slice. L, left; R, right (98).

Figure 6. (A) Brain regions showing significant metabolic changes from pre- to posttreatment in responders of the active transcranial direct current stimulation (tDCS) group compared with the sham tDCS group and in (B) nonresponders of the active tDCS group compared with the sham tDCS group. Significant clusters are overlaid onto an MNI-152 brain template image. The warm color scale indicates increased metabolism and the cool color scale indicates decreased metabolism. The labels of each slice indicate the *z*-coordinate for axial slices. L, left; R, right.

Figure 7. Brain regions showing correlations between observed metabolic changes following transcranial direct current stimulation (tDCS) and tDCS efficacy. Significant clusters are overlaid onto an MNI-152 brain template image. The warm color scale indicates a positive correlation and the cool color scale indicates a negative correlation. The labels of each slice indicate the *z*-coordinate for axial slices and the *x*-coordinate for the sagittal slice.L, left; R, right (98).

Figure 8. Brain regions showing correlations between observed metabolic changes following transcranial direct current stimulation tDCS and baseline gray matter volume. Significant clusters are overlaid onto an MNI-152 brain template image. The warm color scale indicates a positive correlation and the

cool color scale indicates a negative correlation. The labels of each slice indicate the *z*-coordinate for axial slices and the *x*-coordinate for the sagittal slice.L, left; R, right.

Figure 9. Brain regions showing correlations between observed metabolic changes following transcranial direct current stimulation and scores of Beck Depression Inventroy. Significant clusters are overlaid onto an MNI-152 brain template image. The warm color scale indicates a positive correlation and the cool color scale indicates a negative correlation. The labels of each slice indicate the *z*-coordinate for axial slices. L, left; R, right (98).

1. Introduction

1.1. Mechanisms of neuropathic pain following spinal cord injury

Neuropathic pain, is defined as pain initiated or caused by a primary lesion or dysfunction of the nervous system, is generally chronic and disabling (1, 2). Spontaneous neuropathic pain is often generated in the peripheral nervous system by ectopic discharges of damaged primary afferents with consecutive sensitization of dorsal horn neurons (3). Many patients with neuropathic pain exhibit persistent or paroxysmal pain that is independent of a stimulus. This stimulus independent pain can be shooting, lancinating, or burning. Especially, neuropathic pain is a momentous problem in many patients with spinal cord injury (SCI); it has a prevalence of almost 50% among patients with SCI and leads to greater deterioration of daily activity, sleep, mood, and quality of life than does motor impairment (4, 5).

Neuropathic pain following SCI is divided into at-level and below-level pain, according to the regions of pain that result from SCI (6). At-level pain is a central or peripheral neuropathic pain that occurs in dermatomes near the spinal injury and three dermatomes below this level. It is often characterized as either stabbing or is a stimulus-independent type that is accompanied by allodynia. Below-level pain is refers to central neuropathic pain present in the region more than three dermatomes below the neurological level of injury. It has typical characteristics such as burning, electric or shooting qualities and is often classified as a stimulus independent continuous pain (6, 7).

Central sensitization is an important mechanism of persistent neuropathic pain. After SCI, when the quality of a peripheral stimulus does not change, central mechanisms must account for the observed enhancements in nociceptive processing of dorsal horn neurons. Immediately after a neuronal trauma, excessive glutamate release and the resulting increased neuronal activity may initiate a spinal central sensitization (8). Loss of tonic inhibition by gamma-aminobutyric acid (GABA) interneurons or descending tracts (9, 10), intraspinal sprouting (11), changes in N-methyl-D-aspartate (NMDA) and other ionotropic as well as metabotropic glutamate receptors (12, 13) and abnormal expression of sodium channels (14) may contribute to the plasticity and initiation and maintenance of the spinal sensitization. The resultant changes include an increased background activity and responsiveness to peripheral stimuli, reduced thresholds, expanded receptive fields, and prolonged afterdischarges in dorsal horn neurons (15, 16).

Considering the widespread changes following SCI, it is conceivable that neuronal hyperexcitability in dorsal horn neurons around the spinal injury interact with remote centers to cause and maintain neuropathic pain. More recent studies suggest that microglia could be activated in the spinal cord after clinical and experimental SCI, and contribute to the hyperexcitability of dorsal horn neurons (7, 17). Moreover, SCI triggers upregulation of the neuroimmune modulator, cysteine-cysteine chemokine ligand 21(CCL21), which induces further activation of microglia in the thalamus (7, 18). The microglial activation along the sensory neuraxis as well as site of injury contributes to neuronal hyperexcitability, which is possibly linked to chronic pain after SCI (7, 17-20).

Knowledge about the mechanisms that produce neuropathic pain following SCI has advanced through laboratory investigation and quantitative sensory testing of symptoms of patients. Recently, evidences suggest that persistent pain after SCI associated with alterations in supraspinal pain modulatory mechanisms as well as spinal molecular changes. More profound understand of the mechanisms of neuropathic pain following SCI at the central level will be based on effective treatment.

1.2. Brain structural and functional changes in neuropathic pain

As developing of human neuroimaging techniques, our understanding of the role of the brain in pain processing is increased. The human pain experience is a multidimensional phenomenon with sensory-discriminative, affective-motivational, motor and autonomic components (21). Functional neuroimaging studies about activation in response to pain have consistently been reported evidence for an involvement of the thalamus, insula, prefrontal cortex, and anterior cingulate cortex (ACC) as well as primary (S1) and secondary somatosensory cortex (S2) (22, 23, 24). Nociceptive input into primary and secondary somatosensory cortices at least partially underlies the perception of sensory-discriminative features of pain. In contrast, ACC and anterior insula have been implicated in the affective-motivational processing of pain (21, 25, 26). The prefrontal cortex may be related to cognitive process such as pain related memory or stimulation evaluation (23). The thalamus is one of the main structures that receive projections from multiple ascending

pain pathways; therefore, it could be involved in both sensory discriminative and affective-motivational components of pain (27).

Recent neuroimaging studies have reported reorganization of the pain-related brain regions in chronic neuropathic pain conditions. Firstly, several studies reported changes in basal brain activity in patients with neuropathic pain. Iadarola et al (28) found a decrease in the thalamic blood flow contralateral to the symptomatic side compared to the ipsilateral side in patients with unilateral chronic pain. Hsieh et al (29) investigated the effect of regional nerve block with lidocaine providing significant pain relief on patients with chronic painful neuropathy. Comparisons of regional cerebral blood flow (rCBF) between the patient's habitual pain state and the pain alleviated state revealed that the bilateral anterior insula, posterior parietal cortex, prefrontal cortex, and the right ACC showed decreased rCBF after treatment. These results indicated that the initial level of rCBF were abnormally high in these brain regions. In contrast, the posterior thalamus contralateral to the painful side showed increased rCBF. Egloff et al (30) found significant hypometabolism in the posterior insula, ACC, and pre- and postcetnral gyri in patients with chronic pain disorders.

Anatomical magnetic resonance imaging (MRI) techniques have also shown that chronic pain is associated with structural changes in the brain. One study demonstrated a reduction of gray matter volume in the thalamus and dorsolateral prefrontal cortex (DLPFC) of patients with chronic back pain (31), and another study reported a loss of gray matter volume in the anterior insula and ventromedial prefrontal cortex in patients with complex regional pain syndrome (CRPS) (32). Similarly, Kuchinad et al (33) found that fibromyalgia patients showed a greater age-associated decrease in gray matter, and less

gray matter density in several brain regions including cingulate, insula, and medial frontal cortex than healthy controls.

Furthermore, a study using diffusion tensor imaging (DTI), which allows investigation of the microstructure and integrity of the white matter fiber tracts (34), found that patients with fibromyalgia showed significant white matter changes in a number of brain regions associated with sensory perception and affective dimensions of pain, including the thalamus, prefrontal cortex, insula, amygdala, and postcentral gyrus; moreover these changes were correlated with pain severity in patients with fibromyalgia (35). Geha et al (32) found decreased fractional anisotropy in the left cingulum-callosal bundle connected with ACC in CRPS.

Functional MRI (fMRI) studies have demonstrated disruptions of the default mode network (DMN) (36, 37) in patients with chronic pain. Neuroimaging studies found a set of brain regions that usually decrease their activity during task performance when compared with the average brain activity at rest. The fact that these brain regions were more active at rest than during task performance suggested the existence of a resting state, in which was called the default mode of brain function (38, 39). The brain regions compose of DMN showed high correlation of spontaneous brain activity at rest (40). The brain DMN is disrupted in autism (41), depression (42) and Alzheimer's disease (43), suggesting that the study of resting study activity could be useful to understand underlying neural mechanisms of disease. Baliki et al (36) found that chronic back pain patients displayed reduced deactivation in medial prefrontal cortex, and posterior cingulate cortex (PCC), key regions of DMN during a simple visual reaction task. Napadow et al (37) investigated resting-state fMRI from patients with fibromyalgia and found

greater connectivity within the brain regions of DMN and greater connectivity between DMN and the insula.

The supraspinal changes associated with neuropathic pain following SCI have been much less investigated other types of neuropathic pain, such as chronic back pain or fibromyalgia. Wrigley et al (44) investigated whether the degree of the S1 reorganization following SCI correlated with on-going neuropathic pain intensity. The S1 mapped using fMRI during light brushing of the right litter finger, thumb and lib. The little finger activation moved medially in the patients and the amount of the S1 reorganization was correlated with on-going pain intensity level. Using DTI, Gustin et al (45) found abnormal mean diffusivity in the nucleus accumbens (NAc), orbitofrontal cortex and DLPFC, thalamus, and posterior parietal cortex. The amount of change in all these regions significantly correlated with pain severity.

These evidences suggest that chronic neuropathic pain is associated with structural and functional changes of both gray and white matter, which are involved in broad regions related to pain perception and modulation. However, the patterns of detected brain alterations vary according to the type of neuropathic pain and the method of neuroimaging. Especially, the underlying neural mechanisms of the neuropathic pain following SCI are limited to only studies about S1 and white matter changes. Moreover most of the studies have analyzed the brain changes only specific point of view, structure or function. The assessment of structure-function relationships plays an important role in developing understanding of brain in neuropathic pain. To better understand the neural mechanisms underlying chronic neuropathic pain after SCI and to contribute to development of new treatment for

refractory pain, more extensive neuroimaging studies in neuropathic pain following SCI are necessary

1.3. Treatment of neuropathic pain with non-invasive brain stimulation techniques

Despite a variety of pharmacological, neurosurgical, and behavioral therapeutic strategies, patients with neuropathic pain following SCI often fail to experience sufficient relief (7). Treatment of neuropathic pain is still difficult despite the development of new treatment strategies, and there is no single strategy that works for all conditions and their underlying mechanisms. Until now, treatment of neuropathic pain is generally focused on pharmacological management, such as gabapentine, opioid analgesics, tramadol hydrochloride, and tricyclic antidepressants (1).

Recently, brain stimulation on primary motor cortex (M1) invasively or non-invasively has been suggested promising therapy for patients with refractory pain. Since epidural motor cortex stimulation (MCS) was first proposed by Tsubokawa et al (46), different groups have reported high response rate more than 50% (47, 48). Nguyen et al (47) found significant improvement in almost 80% of patients with neuropathic pain on whom MCS had been used over average 27.3 months. Nuti et al (48) observed more long-term outcome over average 4-year and found that about 50% of patients showed more than 40% of pain relief compared to before MCS treatment. Moreover, pain rating reduced when the stimulator was switched on compared to the off-stimulation condition in a randomized controlled study (49). In several animal studies suggested that the mechanisms of analgesic effects of

MCS are inhibition of afferent transmission in the dorsal horn (50, 51). More precise mechanisms underlying MCS clinical effects have been identified by functional neuroimaging procedure such as positron emission tomography (PET). MCS appears to trigger increased activation in thalamus, ACC, orbitofrontal cortex, insula and brainstem including periaqueductal gray matter (PAG) (42-55). Activation in thalamic nuclei suggested as a first step allowing the pain relieving by MCS would lead to several events in other pain-related structures, such as the ACC, PAG, and spinal cord (52). MCS could influence the affective-emotional component of chronic pain by way of cingulate, prefrontal and anterior insular activation. Moreover, functional connectivity analysis identified significant correlation between the CBF changes of ACC and PAG in the post-MCS period (54). These results suggest that the descending thalamic inhibitory pathway to spinal cord or emotional top-down pain modulatory system, both of them affect to pain relief by MCS (42-56).

Based on evidences of analgesic effect of MCS in previous studies, non-invasive brain stimulation on motor cortex using repetitive transcranial magnetic stimulation (rTMS) and transient direct current stimulation (tDCS) started to investigate for pain relief. rTMS on motor cortex induced a long-lasting decrease in chronic pain in the range of 23-45% (57-59) in central and peripheral neuropathic pain patients. Lefaucheur et al (57) investigated analgesic effect of rTMS over M1 in a series of patients with intractable and chronic neurogenic pain. After a single session of 10 Hz rTMS for 20 minutes, the percentage pain reduction was about 23% in real rTMS group, which was significantly greater than sham stimulation group. It has been identified that repeated application of rTMS could produce long-term therapeutic effect.

Khedr et al (58) found that pain ratings in real rTMS group decreased by 45% compared with baseline measure at the end of the fifth treatment session and was still reduced by 40% two weeks later. Passard et al (59) performed real or sham rTMS over M1 for 10 days in patients with fibromyalgia. They also found that real rTMS significantly reduced pain and improved of quality of life for up to 2 weeks after treatment had ended.

tDCS is another non-invasive brain stimulation technique which is based on the application of a weak direct current to the scalp that flows between two relatively large electrodes, anode and cathode electrodes, for modulation of the level of cortical excitability (60). Although tDCS has different mechanism of action, it induced similar modulatory effects in rTMS. The modulatory effects of tDCS are reversible, painless, and safe. Moreover, tDCS is less expensive, and easier to administer than rTMS (61, 62). Motor cortex anodal stimulation has been reported to be able to increase pain threshold in healthy controls (63), and to relief chronic pain. Patients with chronic pain after SCI were randomized to receive sham or active 2 mA tDCS on motor cortex during 5 days. There was significant pain improvement after active anodal stimulation compared to sham stimulation, 63% of patients showed 50% or more reduction in visual analogue scale (VAS) ratings. They found not only that the effects of consecutive sessions were cumulative, but also that the effects of tDCS lasted for at least 24 h as the pain VAS scores for the post-treatment were not significantly different from those of the pre-treatment on the following day (64). Pain in patients with multiple sclerosis was also relieved after 5 days anodal stimulation and this pain improvement persisted until 3 weeks after tDCS sessions (65). These evidences suggest that

repeated sessions of anodal tDCS over the M1 may be useful for pain relief and may have a long-lasting effect.

In spite of the encouraging results of tDCS, detailed mechanisms accounting for its analgesic effect have not yet been elucidated. It was reported that tDCS over M1 for 10 minute in healthy subjects induced bi-directional rCBF changes in many cortical and subcortical areas, such as the somatosensory cortex, cingulate cortex, frontal and parietal areas and thalamus as well as the motor cortex (66). A recent study using fMRI was found significant decreased activity in the S2, insula, prefrontal cortex and putamen after 5 days rTMS stimulation in patients with central pain after stroke. These changes were only found in rTMS responder (patients with decreased VAS score), not in nonresponder (67). These results imply that the modulation of the distributed pain network mediates pain relief after rTMS on M1 and the effect of stimulation could be depend on individual characteristics even if they have same types of neuropathic pain. To develop more effective protocols of tDCS, it is necessary to research on the underlying neural mechanisms of tDCS analgesic effects and biological factors associated with effectiveness of tDCS.

1.4. Purpose of the study

The present study was, firstly, aimed to contribute to a better understanding of the neural mechanisms underlying chronic neuropathic pain following SCI by using [^{18}F]-fluorodeoxyglucose PET ([^{18}F]FDG-PET) and structural MRI, which would enable to capture functional and anatomical brain characteristics. We investigated whether these different imaging modalities provide complementary information on the brain mechanisms of neuropathic pain following SCI and the functional and structural changes have any relationship.

Secondly, it was investigated the neural mechanisms underlying the effects of tDCS using [^{18}F]FDG-PET. [^{18}F]FDG-PET at rest measures the distribution of glucose uptake, which reflects integrated synaptic activity (68). We conducted [^{18}F]FDG-PET imaging before, and 10 days after applying active or sham motor cortex stimulation using anodal tDCS. This method enabled us to assess which components of the pain network could contribute to pain relief by tDCS.

From the results of these two studies, we could understand the pathomechanisms of neuropathic pain following SCI, and contribute to development of new treatment for refractory pain.

2. Study 1: Cerebral changes associated with neuropathic pain following spinal cord injury

2.1. Methods

2.1.1. Subjects

Sixteen patients with chronic neuropathic pain due to traumatic SCI were recruited for this study. The inclusion criteria were: 1) more than 6 months since SCI, 2) stable chronic pain for at least the 3 preceding months, 3) pain that was not attributable to causes other than neuropathic pain (e.g., musculoskeletal pain or pain from diabetic polyneuropathy), and 4) pain that was resistant to medications, or physical or complementary medical treatment. Patients with any kind of metal implant in the head, heart disease, a cardiac pacemaker, or a family or personal history of epilepsy or neuropsychiatric illness were excluded. The characteristics of SCI-related pain were assessed according to the international spinal cord injury data set (6), and the extent of injury was defined by the American Spinal Injury Association (ASIA) impairment scale (69). Because depression is a common comorbidity in patients with chronic neuropathic pain (70), the Beck Depression Inventory (BDI) was completed for all patients. All patients were being treated with various medications including anticonvulsants, nonsteroidal anti-inflammatory drugs, and antidepressants. They were instructed not to change the dosage throughout the experimental period.

Ten age- and gender-matched healthy subjects (6 males and 4 females, 39.5 ± 8.6 years) were recruited as controls. Healthy control subjects had to be free of any chronic or acute pain, medication and neurological disorder. The

study protocol was approved by the Institutional Review Board of the Seoul National University Bundang Hospital, Korea and written informed consent was obtained from all participants after a detailed explanation of the procedure.

2.1.2. Image acquisition

[^{18}F]FDG-PET images were acquired using an Allegro PET scanner (Phillips Medical System, Cleveland, Ohio, USA) operating in three-dimensional (3D) mode. All subjects had fasted for at least 6 hours before scanning. They received an intravenous injection of 4.8 MBq/kg of FDG in a quiet, dimly lit waiting room and were instructed to remain lying comfortably during an FDG equilibration period of 40 minutes. Ten-minute emission scans and attenuation maps using a Cs^{137} transmission source were obtained. Attenuation-corrected images were reconstructed using the 3D Row-Action Maximum-Likelihood algorithm with a 3D image filter of 128 × 128 × 90 matrices with a pixel size of 2 × 2 × 2 mm.

High-resolution T1-weighted structural images were acquired using a 3.0 T MR system (Achieva, Philips Medical Systems, Best, the Netherlands). The 3D T1-weighted turbo field echo (T1TFE) sequence used the following parameters: TR = 8.1 ms, TE = 4.6 ms, flip angle = 8°, 175 slices, thickness = 1 mm, and matrix size = 256 × 256.

2.1.3. Data processing

2.1.3.1. FDG-PET data

FDG-PET images were processed and analyzed using SPM8 (Statistical Parametric Mapping, Wellcome Department of Cognitive Neurology, London, UK) running on Matlab 7.6 (The Mathworks, MA, USA). Original FDG-PET images were corrected for a partial volume effect (PVE) based on a modified version of the Müller-Gärtner approach, which was fully implemented in the PVElab software package (http://pveout.area.na.cnr.it/) (71). Individual FDG-PET images were coregistered to structural MR images, and then MR images were normalized to a T1-weighted MRI template developed and distributed by the Montreal Neurological Institute (MNI). By using these parameters, FDG-PET images were normalized and reformatted with a voxel size of 2 × 2 × 2 mm. The normalized PET images were then smoothed with a 12-mm FWHM isotropic Gaussian kernel.

2.1.3.2. Structural MRI data

Voxel-based morphometry (VBM) (72) was performed using SPM8 with the DARTEL algorithm implemented in Matlab 7.6. Each anatomical MR image was first re-oriented parallel to the plane of anterior and posterior commissures, and then segmented to different tissue types using the new segment option. Using the DARTEL nonlinear image registration procedure (73), segmented gray matter images were aligned to the gray matter average template and then transformed to MNI spaces. The spatially normalized gray matter images were then rescaled by the Jacobian determinants of the deformations in order to preserve relative tissue volumes. Finally, the

normalized and modulated gray matter images were smoothed using a 12-mm FWHM Gaussian filter.

2.1.4. Statistical analyses

2.1.4.1. Group comparisons

Statistical analyses to evaluate the changes of brain glucose metabolism and gray matter volume in patients compared to healthy controls were performed using the two-sample *t*-test of SPM8. Regional glucose metabolism at each voxel of the [^{18}F]FDG-PET image was proportionally scaled into the mean FDG uptake value of the pons. Age was included as a covariate of no interest. For VBM analysis, age and total intracranial volume for controlling different individual head size were included as covariates of no interest. Since corrections for multiple comparisons are typically conservative, and we had a relatively small number of subjects, we set the threshold to $p < 0.001$, uncorrected, for both [^{18}F]FDG-PET and VBM analyses. Since such an uncorrected threshold might result in false-positive differences, for those areas which passed this threshold, a small volume correction (SVC) for multiple comparisons was then applied, setting the cut-off value for significance at $p < 0.05$ and using a sphere of 10-mm radius. Only those areas that passed this additional correction were reported.

2.1.4.2. Effect of disease characteristics on brain changes

After initial assessment of group comparisons, post hoc exploratory analyses were performed to examine potential effects of disease characteristics, such as ASIA classification, level of SCI, months since SCI, pain intensity and scores of BDI and baseline NRS, on brain changes. For these analyses, we extracted

average regional metabolism, and gray matter volume from the significant clusters of each brain imaging analysis. For categorical variables (ASIA classification and level of SCI), we dichotomized the brain regional values into two groups and compared them using the Mann–Whitney U test. The correlations between brain regional values and continuous variables (months since injury, scores of BDI and baseline NRS) were tested using the Pearson correlation. The Mann-Whitney U test and Pearson correlation test were performed using SPSS 13.0.

2.1.4.3. Relationships between brain changes of metabolism and gray matter volume: ROI-based

In order to investigate the relationships between brain changes in patients obtained using different imaging modalities, multiple regression analyses using SPM8 were performed to correlate regional values derived from significant clusters for a specific modality with whole brain imaging of the other modality. To evaluate relationships between brain glucose metabolism and gray matter volume in patients, firstly, the mean value of significant clusters of VBM analysis served as covariates, during which voxels on [^{18}F]FDG-PET images showing significant correlations with the covariates were searched for within whole brain. Gray matter images were also analyzed in the same manner with [^{18}F]FDG-PET images. For these analyses, we set the threshold to $p < 0.005$, uncorrected for multiple comparisons. We used more liberal statistical threshold compared to group *t*-test, for searching trend of correlations.

2.1.4.4. Relationships between brain changes of metabolism and gray matter volume: Parallel ICA

The conventional ROI-based correlation analysis is generally limited to studies of localized relationships. To overcome this limitation, we turned to the concept of parallel independent component analysis (ICA), an effective method for joint analysis of multimodal imaging data. These methods belong to blind source separation approaches, as they do not require prior hypotheses about the connection of interest (74). Parallel ICA identifies independent components of both modalities and connections between them through enhancing intrinsic interrelationship (75). To obtain statistical maps of joint relationships, we used Fusion ICA Toolbox (http://mialab.mrn.org/software/fit). In the context of this study, the parallel ICA design identified spatially independent component (IC) in each imaging modality while simultaneously revealing the disease specific component and the correlation of these component between different modalities. Using the improved minimum description length (MDL) criterion (76), the number of IC was estimated for each dataset. For each modality, the loading parameters expressing the contribution of each IC to the variance across subjects were estimated. Each IC for each modality was scaled to unit standard deviation, yielding z-score maps. All component maps were thresholded at a z-score level of $|Z| \geq 2.3$ (99% cumulative probability) for visualization purposes. Two sample t-tests were performed for each IC on its loading parameters between groups. Then, the Pearson's correlation coefficients between loading parameters for only ICs showed difference between groups were used to identify significant relationships between regional brain metabolism and brain atrophy.

2.2. Results

2.1.1. Patient characteristics

The characteristics of patients are listed in Table 1. The subdivision of active or sham tDCS group was for study 2. All sixteen patients participated in the study 1. All patients had characteristics of neuropathic pain (pricking, tingling, hot burning, stabbing, shooting, etc.) below the level of the SCI at multiple sites in their bodies. There were no significant statistical differences in age and gender between patients and healthy controls (age, $p = 0.199$; gender, $p = 0.664$). However, patients showed significantly higher BDI scores compared to controls (3.7 ± 3.7 vs.15.8 ± 8.4, $p < 0.001$). As defined by BDI, 9 patients showed mild depressive symptoms (BDI=10-18) and 4 patients showed moderate to severe depressive symptoms (BDI > 19). However, according to the Diagnostic and Statistic Manual of Mental Disorder IV, none of the participants had major depression or any other psychiatric disease.

Table 1. Characteristics of patients with chronic neuropathic pain following spinal cord injury.

Patient	Sex	Age(yr)	Level of SCI	ASIA	Months since injury	Pain location	BDI	NRS	
								Pre-tDCS	Post-tDCS
Active tDCS group									
1	M	53	C5/C5	A	27	Both arms/hands	11	7	5
2	M	39	T5/T5	A	19	Both legs/feet	17	8	8
3	M	40	T11/T11	A	8	Both feet	27	8	8
4	F	48	C5/C7	B	21	Both lower back /buttocks/legs/feet	15	7	4
5	F	37	T6/T6	B	21	Both buttocks/legs/feet	16	8	6
6	F	36	C6/C6	A	26	Both elbows/hands/lower leg/feet	32	7	5
7	M	40	T10/T10	A	11	Both legs/feet	16	8	8
8	M	34	C5/C5	A	11	Both arms/hands/ knees/feet	4	7	5
9	M	57	C4/C4	B	136	Both arms/hands/ legs/feet	4	8	3
10	M	31	C4/C4	B	22	Both forearms/ hands/lower back	13	8	7
Mean±SD		41.5±8.5			30.2±37.7		15.5±8.8	7.6±0.5	5.9±1.8
Sham tDCS group									
1	M	62	T11/T11	A	59	Both buttocks/legs/feet	20	9	9
2	F	39	T10/T10	A	22	Both buttocks/legs/feet	12	6	4
3	M	48	T11/T11	A	17	Both buttocks/thighs	16	6	5
4	M	45	C5/C5	B	22	Both lower back /buttocks/legs/feet/ hands	30	8	8
5	M	47	C4/C4	A	19	Both arms/hands buttocks/legs/feet	5	7	7

6	M	49	T5/T5	B	10	Both legs/feet	15	7	6
Mean±SD		48.3±7.6			24.8±17.3		16.3±8.4	7.2±1.2	6.5±1.9
Overall Mean±SD		44.1±8.6			28.2±31.0		15.8±8.4	7.4±0.8	6.1±1.8

2.2.2. Changes of regional metabolic activity in patients with neuropathic pain following SCI

A group comparison of regional brain glucose metabolism between patients with neuropathic pain following SCI and healthy controls identified decreased metabolism in the bilateral medial frontal gyrus. No region was found to have increased glucose metabolism (Figure 1A, Table 2).

2.2.3. Gray matter volume changes in patients with neuropathic pain following SCI

A group comparison using VBM analysis identified decreases in gray matter volume in patients with neuropathic pain following SCI. The patients showed a significant volume loss in the left inferior frontal gyrus and right superior frontal gyrus. These regions were part of the DLPFC. Our VBM analysis did not show increased gray matter volume in any brain region (Figure 1B, Table 2).

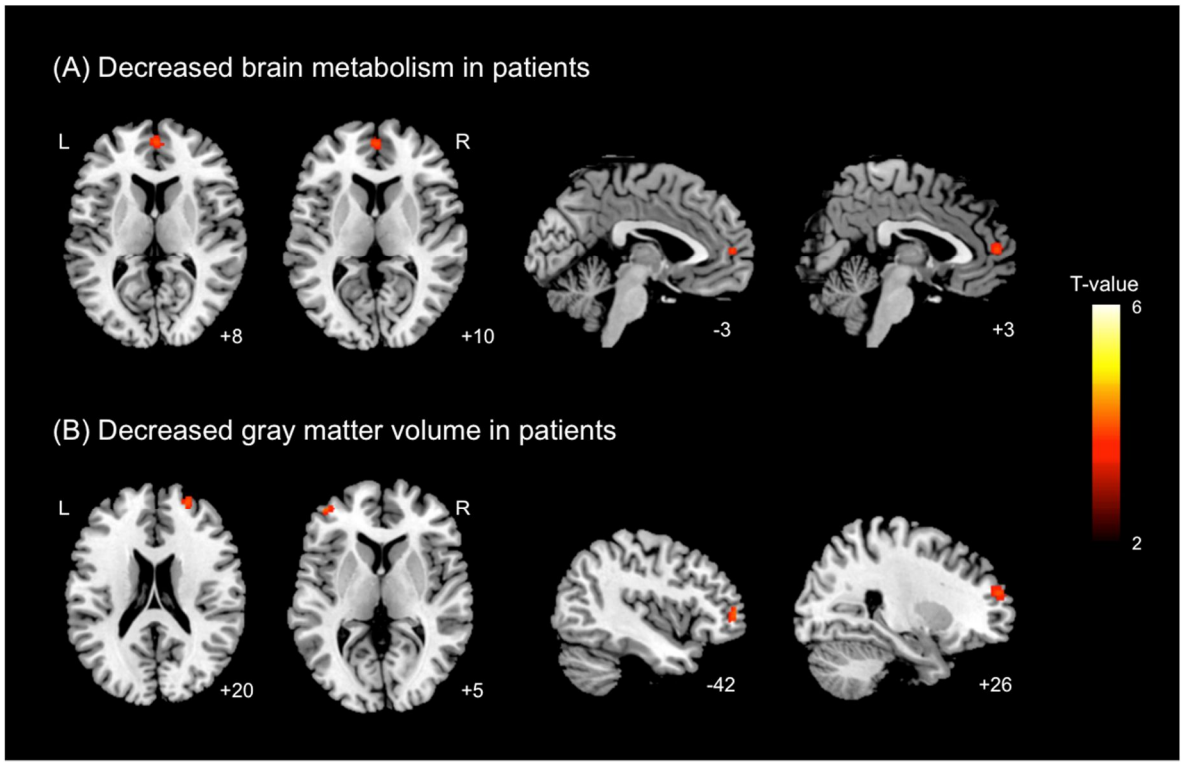

Figure 1. Brain regions showing a significant decrease in (A) brain glucose metabolism and (B) gray matter volume in patients with neuropathic pain following SCI compared to healthy controls. Significant clusters are overlaid onto an MNI152 brain template image. The labels of each slice indicate the *z*-coordinate for axial slices or *x*-coordinate for sagittal slices. L, left; R, right.

Table 2. Brain regions showing significantly decreased metabolism and gray matter volume in SCI patients with neuropathic pain.

Region	Brodmann area	MNI coordinates			t-score	z-score	Cluster size
		x	y	z			
Decrease in metabolism							
L Medial frontal gyrus	BA 10	0	54	8	3.99	3.44	58
Decrease in gray matter volume							
L Inferior frontal gyrus	BA 10	-42	50	4	4.08	3.51	67
R Superior frontal gyrus	BA 10	24	54	20	4.00	3.45	56

L, left; R, right; BA, brodmann area.

2.2.4. Effect of disease characteristics on brain changes

Brain regional values extracted from the significant clusters identified in each brain imaging analysis, the medial prefrontal cortex for brain glucose metabolism, and the left inferior and right superior frontal cortex for gray matter volume, did not differ according to the ASIA classification (complete or incomplete) or the level of SCI (thoracic or cervical), and did not correlated with months since injury or BDI and baseline NRS scores.

2.2.5. ROI-based inter-modal regression analysis

In order to investigate the relationships between brain changes in patients obtained from different imaging modalities, multiple regression analyses were performed to correlate regional values derived from significant clusters for a specific imaging modality with whole brain images of the other modality. In analysis with [^{18}F]FDG-PET images, we did not find any significant brain regions showed correlation with regional gray matter volume values derived from significant clusters for VBM analysis, the left inferior frontal gyrus or the right superior frontal gyrus. In analysis of gray matter volume images, the PCC and adjacent precuneus showed correlations with the metabolic rate in the medial frontal gyrus (peak MNI coordinate, x = 22, y = -54, z = 8; z-value = 4.46) (Figure 2).

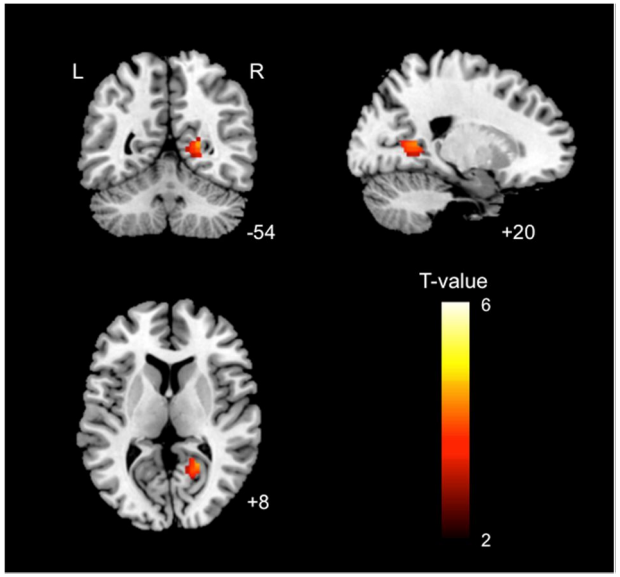

Figure 2. Brain regions in gray matter volume images showing significant negative correlation with medial frontal metabolic rate in patients with neuropathic pain following spinal cord injury. Significant clusters are overlaid onto an MNI152 brain template image. The labels of each slice indicate the *z*-coordinate for axial slice, *x*-coordinate for sagittal slice, or y coordinate for coronal slice. L, left; R, right.

2.2.6. Parallel independent component analysis

Six components for brain metabolic images, and 8 components for gray matter volume images were estimated according to an improved MDL criterion. We found one IC of gray matter volume showing significant difference in loading parameters between groups ($t = 2.45$ $p = 0.02$). The brain regions identified by this component included bilateral DLPFC where showed atrophy in patient group. Additionally, the bilateral precuneus and middle temporal gyrus, and the right medial frontal gyrus and inferior occipital gyrus showed positive values in this component (Figure 3). There were no metabolic ICs showed significant group differences in loading parameters. We performed correlation analysis between the loading parameters with the gray matter component showing group difference and all metabolic components, but there were no significant correlations. However, a metabolic IC including the precuneus and cuneus with positive values and the bilateral superior frontal gyrus with negative values showed a trend towards negative correlation with the gray matter IC (r = -0.36, $p = 0.07$) (Figure 3).

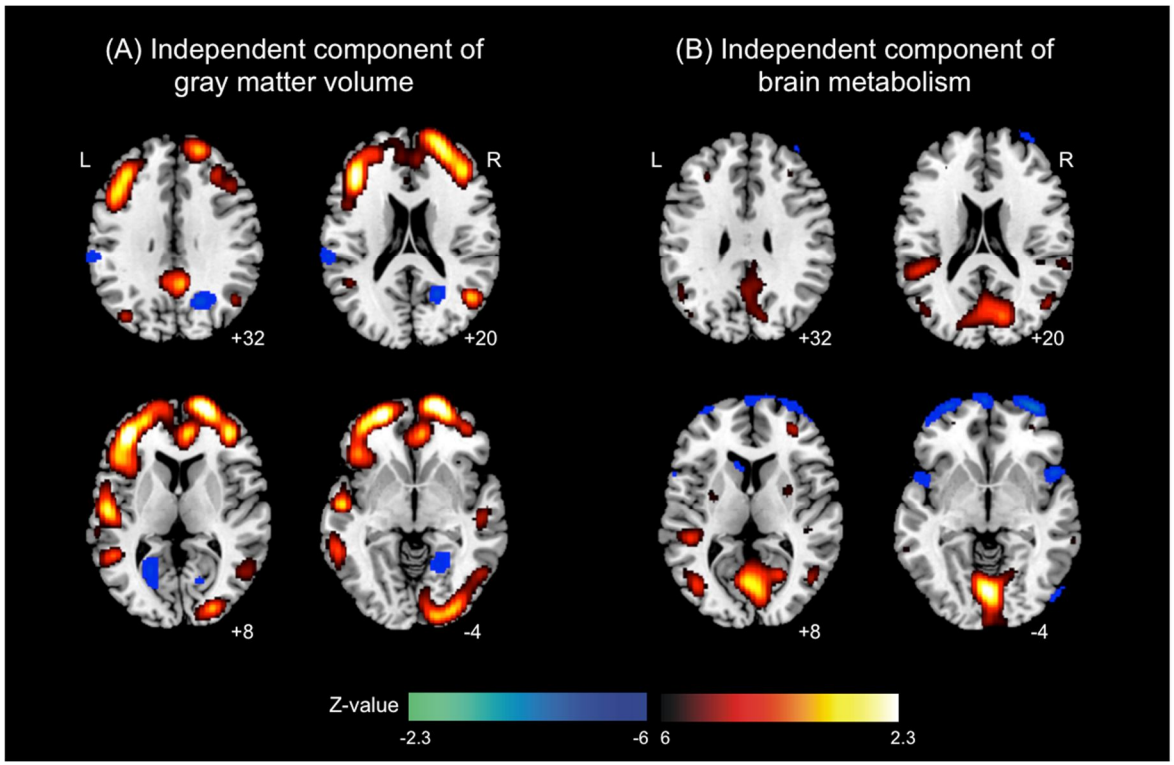

Figure 3. Parallel independent component pair showing a trend towards negative correlation between loading parameters. (A) Independent component of gray matter volume and (b) independent component of brain metabolism. The gray matter component showed significant difference in loading parameters between groups. Significant clusters are overlaid onto an MNI152 brain template image. L, left; R, right.

2.3. Discussion

The study 1 investigated the brain functional and structural alterations and their inter-modal relationships in patients with chronic neuropathic pain following SCI. The results of the present study demonstrated that patients with neuropathic pain following SCI have significant functional and structural abnormalities in the DLPFC and medial prefrontal cortex associated with pain modulation. The ROI-based inter-modal regression analysis revealed the abnormal medial prefrontal metabolism negatively correlated with the gray matter volume in the PCC and precuneus. Additionally, data-driven parallel ICA revealed that gray matter IC including the bilateral DLFPC showed negative correlation with metabolic IC including the precuneus and cuneus. These results suggest that the brain abnormalities in neuropathic pain following SCI related with brain DMN.

The bilateral DLPFC showed decreases in gray matter volume. Atrophy of the DLPFC has been consistently found in previous brain morphometric studies of various chronic pain conditions (31, 77, 78), and previous neuroimaging studies suggested that the DLPFC has a central role in top-down pain processing. In a study of experimentally induced allodynia, DLPFC activation was negatively correlated with unpleasantness as well as perceived pain intensity, supposedly via inhibition of the neuronal coupling between the midbrain and thalamus (79). Another study demonstrated the blockade of placebo analgesia in healthy subjects when the left DLPFC was disrupted by low-frequency rTMS (80). Moreover, a recent study identified that high-frequency rTMS of the left DLPFC leads to reduced allodynia pain ratings, and further found that this analgesia was associated with increased

activity in the DLPFC and decreased activity in the ACC, thalamus, midbrain and medulla (81). Roles of the DLPFC in attention processes (82) and executive function (83) are also believed to related to cognitive modulation of pain processes.

Furthermore, we found hypometabolism in the medial prefrontal cortex. Patients with chronic pain show impairment of emotional decision making, which implies involvement of the medial prefrontal cortex in neural mechanisms of neuropathic pain, since the medial prefrontal cortex is known to modulate emotional evaluation relative to the self (32, 84). Patients with CRPS showed atrophy of the medial prefrontal cortex, and the strength of white matter connectivity between the medial prefrontal cortex and NAc was correlated with heightened anxiety (32). Moreover, recent evidence suggests that the medial prefrontal cortex is important for predicting pain chronification (85, 86). In a longitudinal brain imaging study, subacute back pain patients were followed over the course of 1 year. The persisting back pain patients showed significantly stronger positive connectivity between the NAc and medial prefrontal cortex at both subacute and chronic stages. These results are implying that medial prefrontal cortex is causally involved in the transition from acute to chronic pain. The cortical changes in patients with neuropathic pain following SCI found in the present study were locally different depending on the imaging modalities used but functionally overlapping, which are generally known to participate in pain modulation through affective and cognitive processes. Therefore, the abnormalities in the present study, confirmed by analyses of both cortical volume and metabolism, imply the possibility of disrupted top-down modulatory processing in patients with neuropathic pain following SCI.

Additionally, we found inter-modal negative correlation between brain regions showing abnormal changes in patients and brain regions of DMN, the PCC and precuneus. These results suggest that the brain abnormalities are associated with augmented DMN activity in resting state in neuropathic pain following SCI. It has been proposed that in the normal brain, the DMN is engaged in self-referential thinking that is deactivated during various externally focused task conditions. The increased activity and connectivity within DMN have found in various disorder, such as multiple sclerosis (87), schizophrenia (88), and obese individuals (89). These results imply that the hyperractivity in DMN is associated with disrupted cognitive function or increased focus on internal states. Previous studies have found disrupted DMN network in chronic back pain patients (36) and fibromyalgia (37). FMRI and neurophysiology studies have shown that attention and distraction related modulation of nociceptive driven activations in many brain regions participating pain processing, with concomitant changes in pain perception (90, 91). A clinical feature of many chronic pain patients is hypervigilence to pain and pain-related information. This has a direct impact not only on their resultant pain perception but also quality of life if it impacts cognitive performance (92). Therefore, we could predict that the abnormal brain regions associated with pain modulation have interaction with brain regions of DMN, and it might be associated with enhanced attention to pain and focus on internal states.

Pain is a multidimensional phenomenon with sensory-discriminative, affective-motivational, and cognitive-evaluative components (21). In study 1, we showed that different imaging modalities commonly identified the possibility of deficits in pain modulation by cognitive and emotional

processes in patients with neuropathic pain following SCI. Moreover, these abnormal brain changes had correlation with brain regions of DMN, which suggest that the fail of pain modulation in patients associated with hypervigilence to pain and increased focus on internal states.

2.4. Limitations and suggestions for further studies

The current study has some limitations that may be addressed in future studies. Because we compared patients with neuropathic pain following SCI to healthy controls, rather than to patients with SCI without pain, it may not be possible to completely distinguish between the effects of SCI and effects of pain. In addition, our study used a relatively small patient group that may be somewhat heterogeneous, as assessed by the level of injury and ASIA classification. Nevertheless, our patients had relatively homogeneous pain ratings and pain duration compared to patients with neuropathic pain in other neuroimaging studies. Furthermore, the observed brain changes did not differ according to the patient characteristics. Comparisons between SCI patients without pain and SCI patients with pain who have homogeneous disease characteristics are needed to replicate and refine our findings.

3. Study 2: Underlying neural mechanisms of analgesic effects of tDCS over primary motor cortex

3.1. Methods

3.1.1. Subjects

Sixteen patients with chronic neuropathic pain due to traumatic SCI who recruited in the study 1 also participated in the study 2. The characteristics of patients are listed in Table 1. To control the placebo effect, the patients were assigned to the active or sham stimulation group according to the order of enrollment. The study protocol and consent forms were reviewed and approved by the Institutional Review Board of the Seoul National University Bundang Hospital, Korea. Written informed consent was obtained from all participants after a detailed explanation of the procedure.

3.1.2. Transcranial direct current stimulation

Direct current was delivered by a battery-driven, constant-current stimulator (Phoresor II Auto Model No. PM850, IOMED, Salt Lake City, Utah) via a pair of rubber pads with sponge-insert electrodes. The anode electrode was placed over the left M1 (C3, EEG 10/20 system) and the cathode electrode over the contralateral supraorbital area. This electrode position has been shown to be effective in enhancing the excitability of the M1 (93). For patients with symmetric pain, the stimulation was applied over the dominant hemisphere (57, 64). In our study, all of the patients had symmetric pain and were right-handed, so we stimulated C3. A constant 2 mA current was applied for 20 minutes. Each patient received 20 treatments over a 2-week period.

Treatments were given twice daily, with an interval of more than 4 hours, from Monday to Friday. For sham stimulation, the electrodes were placed in the same positions as for anodal M1 stimulation, but the stimulator was turned off after 10 seconds. Therefore, the patients felt an initial itching sensation, but received no current for the remaining stimulation period (64, 94).

3.1.3. Outcome measures

The numeric rating scale (NRS) score for average pain during the preceding 24 hours was defined as the primary outcome measure. Patients were asked to rate their pain, indicating the number that best described their pain from 0 (no pain) to 10 (the most intense pain sensation imaginable) (95). As a secondary outcome measure, we assessed the patient global impression of change (PGIC) and pain interference. The PGIC is a single-item rating by participants of their improvement after treatment on a 7-point scale that ranges from 1 (very much improved) to 7 (very much worse) with 4 (no change) as the midpoint (96). Each participant was asked to rate how their pain interfered with general daily life, mood, or sleep over the previous week using a 7-point NRS ranging from 0 (no interference) to 6 (complete interference). The NRS for pain intensity and for pain interference was assessed before treatment and the day after treatment, and the PGIC was evaluated on the day after treatment. All evaluations were performed by a rater who was blinded to the study procedures.

3.1.4. Image acquisition

[^{18}F]FDG-PET was conducted twice, on the day before the beginning of the tDCS sessions and the day after the end of treatment. The baseline [^{18}F]FDG-

PET images were same images used in the study 1 and the second [^{18}F]FDG-PET images acquired using the same protocol of baseline PET. The same structural MRI with study 1 also used for anatomical information. The MRI scan was also performed on the day before the beginning of the tDCS sessions.

3.1.5. Data processing

PET and MRI images were processed and analyzed using SPM8 running on Matlab 7.6. Original FDG-PET images were corrected for a PVE using the same method of study 1 and then, images from each patient were realigned to the first PET scan. Then, the PET images were coregistered, spatially normalized and smoothed using the same procedure of study 1. The same spatially normalized, modulated and smoothed gray matter images with study 1 were used in study 2.

3.1.6. Statistical analysis

Between active tDCS group and sham tDCS group, baseline homogeneity of groups was compared by independent *t*-test for continuous variables and Fisher's exact test for categorical variables.

3.1.6.1. Comparisons of pain scores and brain metabolism between before and after tDCS

The effect of tDCS on changes in NRS scores for pain and pain interference was analyzed using the Wilcoxon signed-rank test for each group. A flexible factorial model in SPM8 with group (real and sham) and treatment (pre- and posttreatment) factors was used for the analysis comparing the effect of

treatment on brain glucose metabolism. To identify significant between-group differences in the effect of treatment, paired *t*-tests were performed for each group separately.

3.1.6.2. Changes of brain metabolism in response to tDCS

It is suggested that patients with reductions in NRS of approximately 2 points or 30% from baseline represented a clinically important difference (95). To evaluate the difference in metabolic changes between responder and nonresponder, participants whose NRS score decreased more than two points after active tDCS were classified as responders, and participants whose NRS score decreased less than 2 points were classified as nonresponders. Between responders and nonresponders, baseline homogeneity of groups was compared by Mann-Whitney test for continuous variables and Fisher's exact test for categorical variables. For responders and nonresponders respectively, flexible factorial models in SPM8 with group (real and sham) and treatment (pre- and posttreatment) factors were used. The contrast of pre- and post-sham tDCS used as an exclusive mask to confirm only effect of active tDCS.

Additionally, to detect correlation between brain metabolic changes in the active tDCS group and tDCS efficacy, voxel-by-voxel multiple regression analysis was performed using tDCS efficacy for the difference maps (subtraction from post- to pre-tDCS images). The tDCS efficacy was calculated with the following equation: [(pre-tDCS – post-tDCS pain score)/pre-tDCS pain score × 100]. Brain glucose metabolism at each voxel was proportionally scaled to the mean FDG uptake value of the whole brain.

3.1.6.2. Effect of baseline gray matter volume to the changes of brain metabolism after active tDCS

To assess whether baseline gray matter volume affect to the changes of regional metabolism after tDCS, we performed voxel-to-voxel multi-modal regression between difference maps of [^{18}F]FDG-PET images and baseline gray matter volume using biological parametric mapping (BPM) (97). When comparing across imaging modalities, most studies have been forced to rely on simple ROI type analyses, which do not allow the voxel-by-voxel comparisons to answer the overall effect of biological information from another imaging modalities. The BPM analysis is designed to take imaging data as a covariate in a manner consistent with traditional SPM. In BPM, both the outcome variables and the explanatory variables may be images, each voxel has a different design matrix.

The level of statistical significance for all brain imaging analyses was $P < .005$ without correction. We used a liberal significance threshold to avoid type II errors because the relatively low number of subjects in this study leads to fairly conservative testing.

3.2. Results

3.2.1. Patients characteristics

Patient characteristics are shown in Table 1. There were no significant differences in demographical and clinical characteristics between the active and sham tDCS groups (gender, p =1.0; age, p = 0.127; injury of SCI, p = 0.608; ASIA, p = 1.0; months since injury, p = 0.750; BDI, p = 0.855; baseline NRS, p = 0.319).

3.2.2. Changes in pain intensity after tDCS

The Wilcoxon signed-rank test for each group found a significant decrease in NRS for pain in the active tDCS group (z = –2.410, p = 0.016), but not in the sham tDCS group (p = 0.102). In the active tDCS group, pain intensity was reduced from 7.6 ± 0.5 at baseline to 5.9 ± 1.8 after the tDCS sessions, an average decrease of 22.9%. Seven patients showed various degrees of pain reduction according to NRS data (range, 1–4 or 12.5–62.5%); the NRS scores for the other 3 patients did not change (Table 3).

3.2.3. Patient global impression of change in pain after tDCS

There was no significant difference between the active and sham groups in PGIC score. The average PGIC score in the active tDCS group was 3.7 ± 1.4, which means that patients generally rated the pain-relieving effect of the treatment as ‘no change’. Two patients, who had an improvement in NRS more than 40%, rated pain as markedly improved (‘much improved’ or ‘very much improved’). The other 5 patients reported ‘no change’ in their pain, and 1 patient rated pain as ‘minimally improved’. On the other hand, 2 patients

rated their pain as worse than before ('minimally worse' and 'much worse'). The average PGIC score in the sham tDCS group was 4.3 ± 0.8. In the sham group, 5 patients reported 'no change' in their pain and the sixth rated pain as much worse than before (Table 3).

3.2.4. Changes in pain interference with activities of daily life after tDCS

In the active tDCS group, patients rated pain interference with general daily life as somewhat alleviated after tDCS treatment (4.6 ± 0.8 at baseline; 3.7 ± 0.8 the day after tDCS; $z = -2.251$, $p = 0.024$). However, there were no effects of tDCS on pain interference with mood (3.8 ± 1.4; 3.2 ± 1.3; $p = 0.380$) or sleep (3.7 ± 1.3; 2.8 ± 1.1; $p = 0.135$). In the sham tDCS group, there were no effects of tDCS on pain interference with daily life (2.8 ± 2.5; 3.5 ± 2.1; $p = 0.461$), mood (3.8 ± 2.3; 3.7 ± 1.4; $p = 0.785$), or sleep (2.5 ± 2.8; 1.2 ± 2.4; $p = 0.285$) (Table 3).

Table 3. Response to tDCS of patient with neuropathic pain following SCI.

Patient	NRS			PGIC	Pain interference					
					General daily life		Mood		sleep	
	pre	post	%		Pre	Post	Pre	Post	Pre	post
Active tDCS group										
Responders										
1	7	5	28.6	3	4	4	4	4	4	3
4	7	4	42.9	2	5	3	4	3	4	0
6	7	5	28.6	4	4	3	3	3	3	3
8	7	5	28.6	4	5	3	5	1	5	3
9	8	3	62.5	1	3	3	1	2	1	3
Mean±SD	7.2 ±0.4	4.4±0.9	38.2±14.9	2.8±1.3	4.2±0.8	3.2±0.4	3.4±1.5	2.6±1.1	3.4±1.5	2.4±1.3
Nonresponders										
2	8	8	0	5	5	5	4	5	4	2
3	8	8	0	4	6	5	6	5	4	3
5	8	6	25	6	4	4	3	4	3	4
7	8	8	0	4	5	4	5	2	6	4
10	8	3	12.5	4	5	3	3	3	3	3
Mean±SD	8.0±0.0**	7.4±0.9	7.5±11.2	4.6±0.9	5.0±0.7	4.2±0.8	4.2±1.3	3.8±1.3	4.0±1.2	3.2±0.8
Total	7.6±0.5	5.9±1.8*	22.9±20.4	3.7±1.4	4.6±0.8	3.7±0.8*	3.8±1.4	3.2±1.3	3.7±1.3	2.8±1.1

Sham tDCS group										
1	9	9	0	4	0	5	3	3	0	0
2	6	4	33.33	4	5	3	6	2	6	1
3	6	5	16.67	4	3	3	3	3	4	0
4	8	8	0	6	3	6	6	6	5	6
5	7	7	0	4	0	0	5	4	0	6
6	7	6	14.29	4	6	4	0	4	0	0
Mean±SD	7.2±1.2	6.5±1.9	12.9±13.5	4.3±0.8	2.8±2.5	3.5±2.1	3.8±2.3	3.7±1.4	2.5±2.8	1.2±2.4

NRS, numeric rating scale; PGIC, patient global impression of change; * $p < 0.05$ compared with pre-tDCS;
** $p < 0.05$ compared with responders.

3.2.5. Changes of brain regional metabolism in response to tDCS

A flexible factorial model identified bidirectional metabolic changes from pre- to posttreatment in the active tDCS group compared with the sham tDCS group (Figure 5, Table 4). Significantly increased metabolism after active tDCS compared with sham tDCS was found in the left postcentral gyrus around the stimulation site, the right caudate, and the medulla. Significantly decreased glucose metabolism after active tDCS compared with sham tDCS was found in the left angular gyrus, PCC, and orbital and dorsolateral portions of the left middle and superior frontal gyrus. To interpret the interaction findings, we examined the effect of treatment for the groups separately. In agreement with the interaction results, significantly increased metabolism was observed in the left postcentral gyrus, right caudate, and medulla, and decreased metabolism in the left DLPFC and PCC after active tDCS (Figure 5A, Table 5). For the sham tDCS group, the increased metabolism in the left orbital part of the middle frontal gyrus and the angular gyrus agreed with interaction results (Figure 5B). The changes seen in the PCC and angular gyrus in a separate group analysis were found at a less stringent statistical threshold ($p = 0.01$; data not shown).

Metabolic changes induced by active tDCS were found in additional brain regions. We found increased metabolism in the bilateral hippocampal and parahippocampal areas and the adjacent fusiform gyrus, subgenual ACC (sACC), insulae, left putamen, and brainstem, and decreased metabolism in the right precuneus, and bilateral superior frontal gyri that corresponds to the medial prefrontal cortex after active tDCS (Figure 5A, Table 5). In the sham tDCS group, there was increased metabolism in the left pre-and postcentral

gyrus, right middle and superior temporal gyrus, and right parahippocampal gyrus, and decreased metabolism in the cerebellum (Figure 5B).

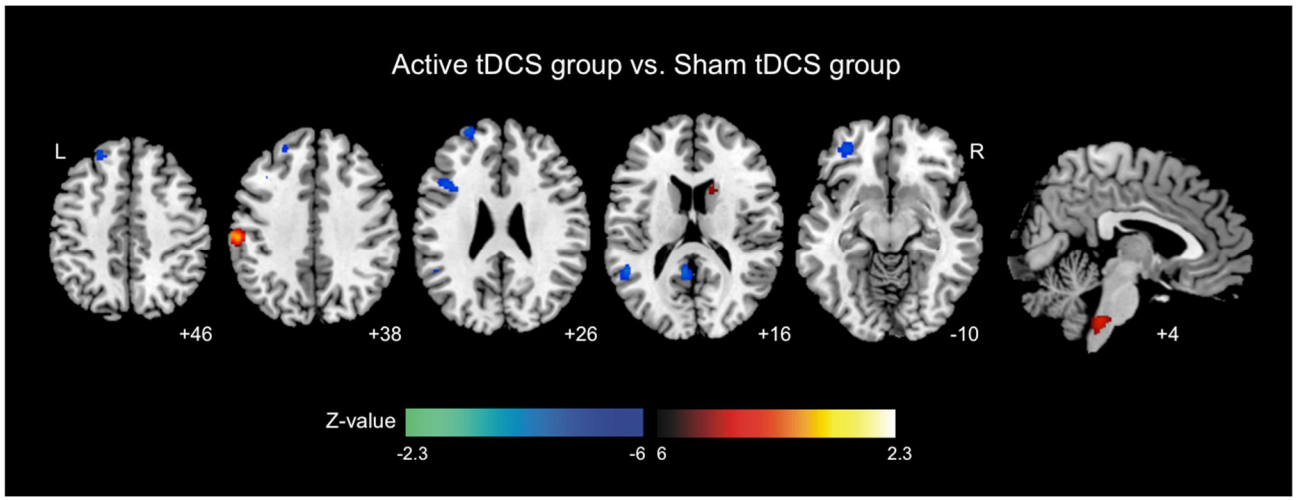

Figure 4. Brain regions showing significant metabolic changes from pre- to posttreatment in the active transcranial direct current stimulation (tDCS) group compared with the sham tDCS group. Significant clusters are overlaid onto an MNI-152 brain template image. The warm color scale indicates increased metabolism and the cool color scale indicates decreased metabolism. The labels of each slice indicate the *z*-coordinate for axial slices and the *x*-coordinate for the sagittal slice. L, left; R, right (98).

Table 4. Brain regions showing significant changes in metabolism after active tDCS in patients with neuropathic pain following spinal cord injury compared with the sham tDCS group.

Region	BA	MNI coordinates			t-score	z-score	Cluster size
		x	y	z			
Increased metabolism							
L Postcentral Gyrus	3	-60	-22	38	5.72	4.04	106
R Medulla		6	-34	-44	4.32	3.39	94
R Caudate		12	14	12	3.52	2.93	58
Decreased metabolism							
L Angular Gyrus	39	-50	-50	16	4.67	3.57	76
L Posterior Cingulate Gyrus	29	-6	-50	14	4.59	3.53	84
L Middle Frontal Gyrus	9/10/11	-24	56	24	4.31	3.38	167
L Superior Frontal Gyrus	8/9	-22	40	48	3.18	2.71	56

L, left; R, right; BA, brodmann area.

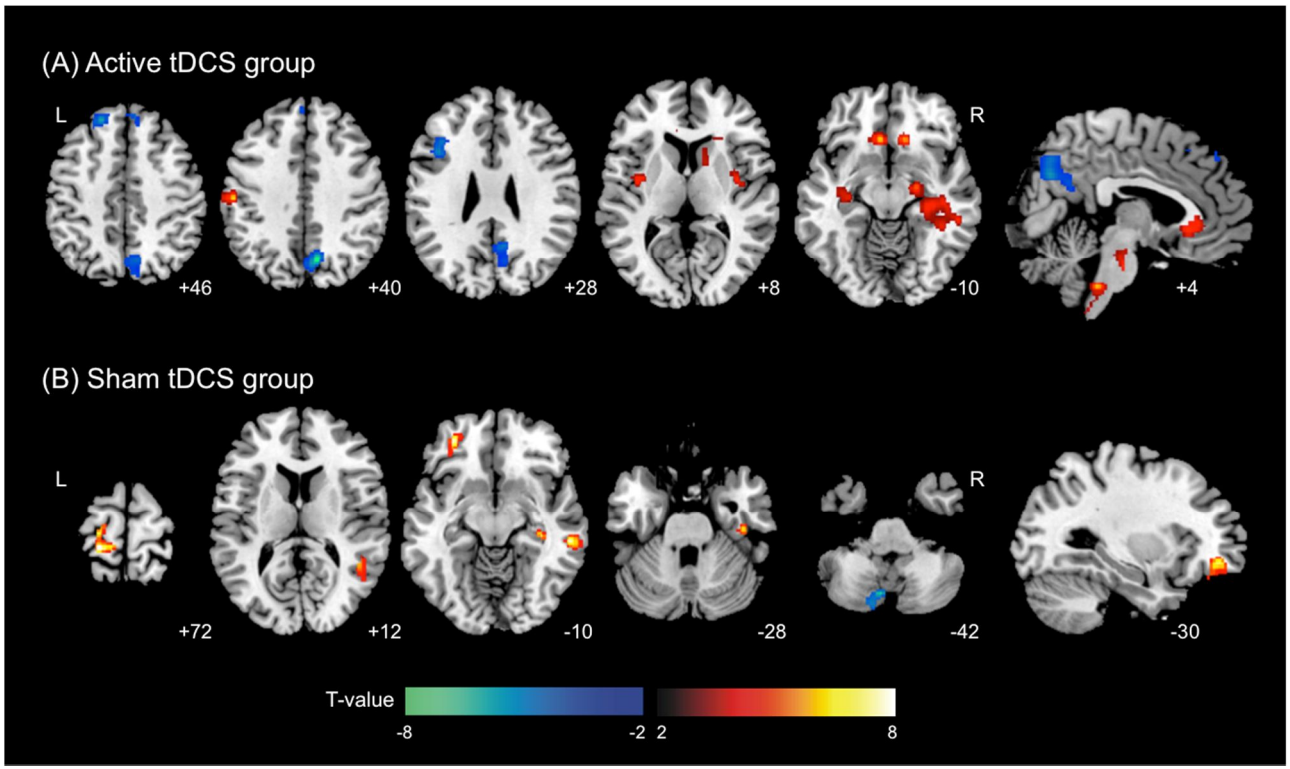

Figure 5. To identify the group whose data accounted for the significant differences in treatment effect, brain metabolic changes were analyzed in each group separately. (A) Significant metabolic changes after active tDCS. (B) Significant metabolic changes after sham tDCS. The labels of each slice indicate the *z*-coordinate for axial slices and the *x*-coordinate for the sagittal slice. L, left; R, right (98).

Table 5. Brain regions showing significant changes in metabolism after active tDCS in patients with neuropathic pain following spinal cord injury.

Region	BA	MNI coordinates			t-score	z-score	Cluster size
		x	y	z			
Increased metabolism							
L Postcentral Gyrus	3	-56	-20	38	7.75	4.18	115
R Parahippocampal Gyrus	28	22	-12	-14	5.15	3.43	1433
R Fusiform Gyrus	20	44	-20	-24	7.66	4.16	
L Parahippocampal Gyrus	35	-30	-26	-26	6.49	3.86	579
L Fusiform Gyrus	20	-40	-14	-28	5.48	3.55	
R Anterior Cigulate Cortex	25	12	24	-10	6.31	3.81	651
L Anterior Cingulate Cortex	25	-6	26	-10	6.31	3.81	997
R Medulla		4	-38	-44	5.91	3.69	84
L Insula	13	-38	-6	8	4.58	3.21	279
L Putamen		-30	-10	2	3.7	2.84	
R Pons		4	-20	-30	4.76	3.28	124
R Midbrain		6	-22	-22	4.5	3.18	
R Insula	13	36	-4	4	4.54	3.19	197
R Middle Temporal Gyrus	38	52	4	26	4.02	2.97	72

Decreased metabolism							
R Precuneus	7	8	-68	36	8.12	4.27	638
L Superior Frontal Gyrus	8	-20	42	48	6.08	3.74	70
L Middle Frontal Gyrus	9	-40	14	26	5.66	3.61	168
R Superior Frontal Gyrus	8	8	42	46	4.71	3.26	76
L Superior Frontal Gyrus	8	-2	48	40	3.91	2.92	

L, left; R, right; BA, brodmann area.

3.2.6. Brain metabolic changes in responders and nonresponders

Of the 10 patients, 6 patients showed decrease in NRS for pain of more than 2 points. However, because one patient who NRS decreased 2 points rated pain as much worse after tDCS treatment on the PGIC, she classified as nonresponder. Therefore, there were 5 responders and 5 nonresponders. The basic characteristics of patients, age, ASIA, months since injury, BDI, did not differ between responders and nonresponders (age, $p = 0.421$; months since injury, $p = 0.151$; BDI, $p = 0.222$). However, responders showed relatively low baseline NRS scores compared to nonresponders ($z = -2.449$, $p = 0.032$) and all the responders had SCI at cervical level, but most nonresponders had SCI at thoracic level ($p = 0.048$).

In comparison to the sham tDCS group, responders showed increased metabolism in cerebellum and decreased metabolism in the right medial frontal gyrus, left superior forntal gyrus and left precunues. Nonrepsonders showed increased metabolism in the right paracentral lobule and left parahippocampal gyrus (Figure 6, Table 6).

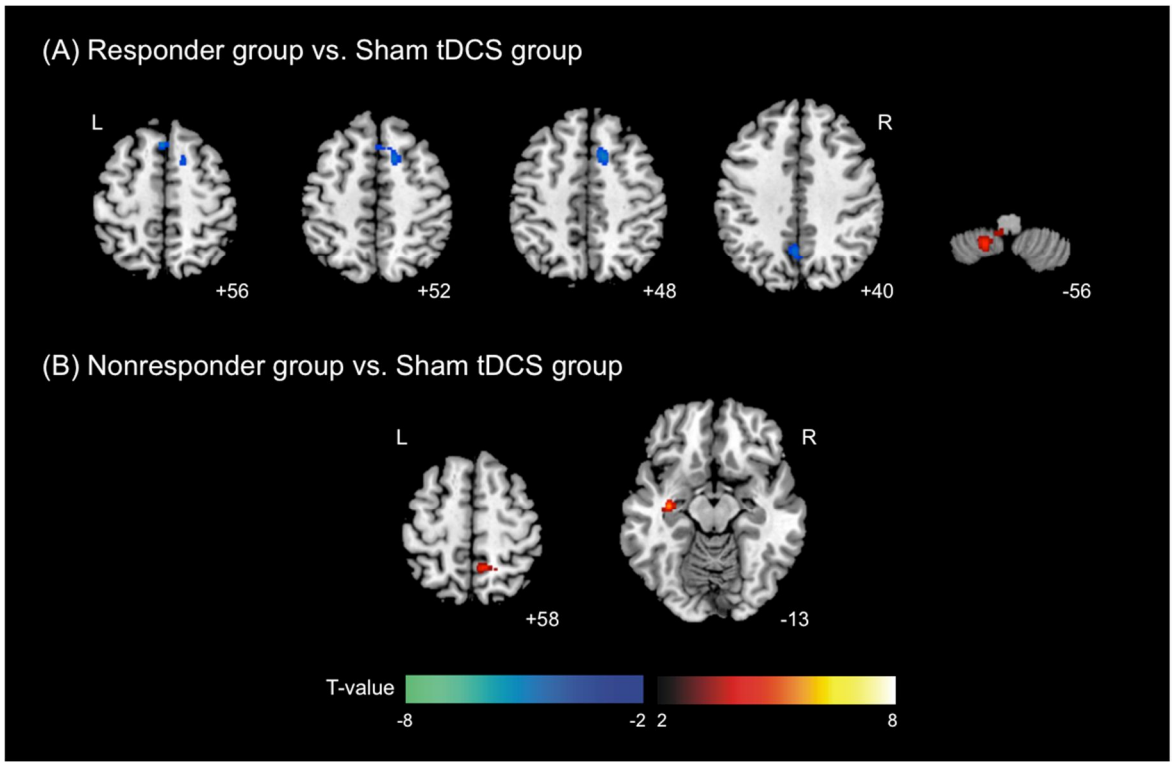

Figure 6. (A) Brain regions showing significant metabolic changes from pre- to posttreatment in responders of the active transcranial direct current stimulation (tDCS) group compared with the sham tDCS group and in (B) nonresponders of the active tDCS group compared with the sham tDCS group. Significant clusters are overlaid onto an MNI-152 brain template image. The warm color scale indicates increased metabolism and the cool color scale indicates decreased metabolism. The labels of each slice indicate the *z*-coordinate for axial slices. L, left; R, right.

Table 6. Brain regions showing significant changes in metabolism in responder and nonresponder groups after active tDCS.

Region	BA	MNI coordinates			t-score	z-score	Cluster size
		x	y	z			
Responders vs. sham tDCS							
Increased metabolism							
L Cerebellum		-18	-50	-60	5.44	3.53	125
Decreased metabolism		6	-34	-44	4.32	3.39	94
R Medial Frontal Gyrus	32	12	14	48	5.30	3.49	158
L Superior Frontal Gyrus	8	-2	22	56	4.79	3.29	
L Precuneus	7	-4	-58	40	4.53	3.19	64
Nonresponders vs. sham tDCS							
Increased metabolism							
L Parahippocampal Gyrus	36	-34	-14	-12	5.52	3.56	89
R Paracentral Lobule	7	8	-50	60	4.33	3.11	115

L, left; R, right; BA, brodmann area.

3.2.7. Correlation between brain metabolic changes and tDCS efficacy

Voxel-by-voxel multiple regression analysis using tDCS efficacy for the difference maps of PET scans was identified both positive and negative correlations. tDCS efficacy was positively correlated with metabolic changes in the bilateral cerebellum and left medulla. The negative correlation was found in the left precuneus and perigenual ACC (pACC), along with the adjacent medial frontal gyrus and the bilateral middle frontal gyri, equivalent to the DLPFC (Figure 7, Table 7).

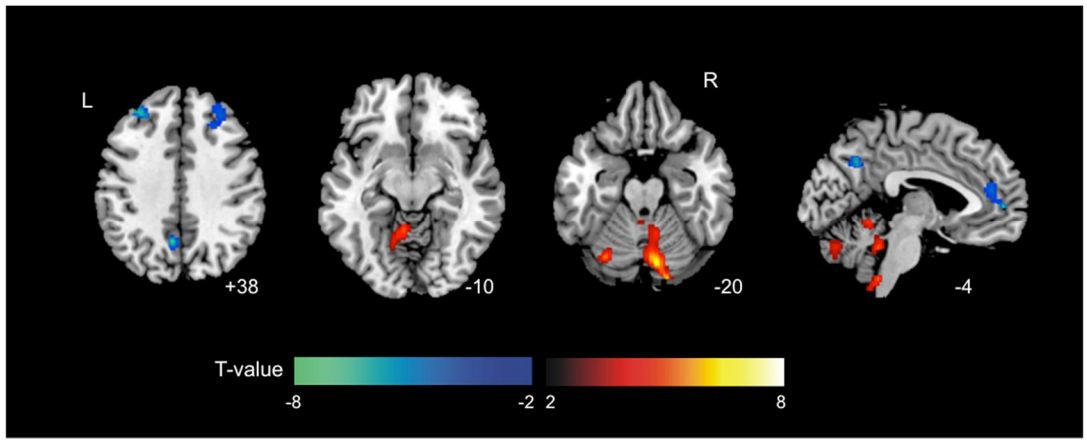

Figure 7. Brain regions showing correlations between observed metabolic changes following transcranial direct current stimulation (tDCS) and tDCS efficacy. Significant clusters are overlaid onto an MNI-152 brain template image. The warm color scale indicates a positive correlation and the cool color scale indicates a negative correlation. The labels of each slice indicate the *z*-coordinate for axial slices and the *x*-coordinate for the sagittal slice.L, left; R, right (98).

Table 7. Brain regions showing correlations between observed metabolic changes following transcranial direct current stimulation (tDCS) and tDCS efficacy.

Region	BA	MNI coordinates			t-score	z-score	Cluster size
		x	y	z			
Positive							
R Cerebellum		10	-76	-20	6.7	3.79	1888
L Medulla		-8	-42	-54	5.67	3.5	
L Cerebellum		-28	-72	-20	5.47	3.43	110
Negative							
L Precuneus	7	-6	-60	38	7.23	3.92	71
L Middle Frontal Gyrus	9	-32	42	40	7.22	3.91	135
L Medial frontal gryus	9	-4	52	4	6.42	3.71	101
L Anterior Cingulate Cortex	32	-2	44	10	4.51	3.09	
R Middle Frontal Gyrus	9	32	36	36	4.32	3.02	129

L, left; R, Right; BA, brodmann area

3.2.8. Relationship between baseline gray matter volume and brain metabolic changes

Significant correlation between difference maps of brain metabolism and baseline gray matter volume were found in several brain regions. The left thalamus including part of the pulvinar, ventroposterior lateral, and lateral posterior nucleus showed positive correlations (Figure 8, Table 8). The positive correlation means that the brain regions have relatively high grey matter volume showed increased metabolism after tDCS. On the other hand, the bilateral precuneus, left middle and superior frontal gyrus, left fusiform gyrus, left insula, right inferior frontal gyrus and right superior parietal lobule showed negative correlations (Figure 8, Table 8). The negative correlation means that the brain regions have relatively high grey matter volume showed decreased metabolism after tDCS.

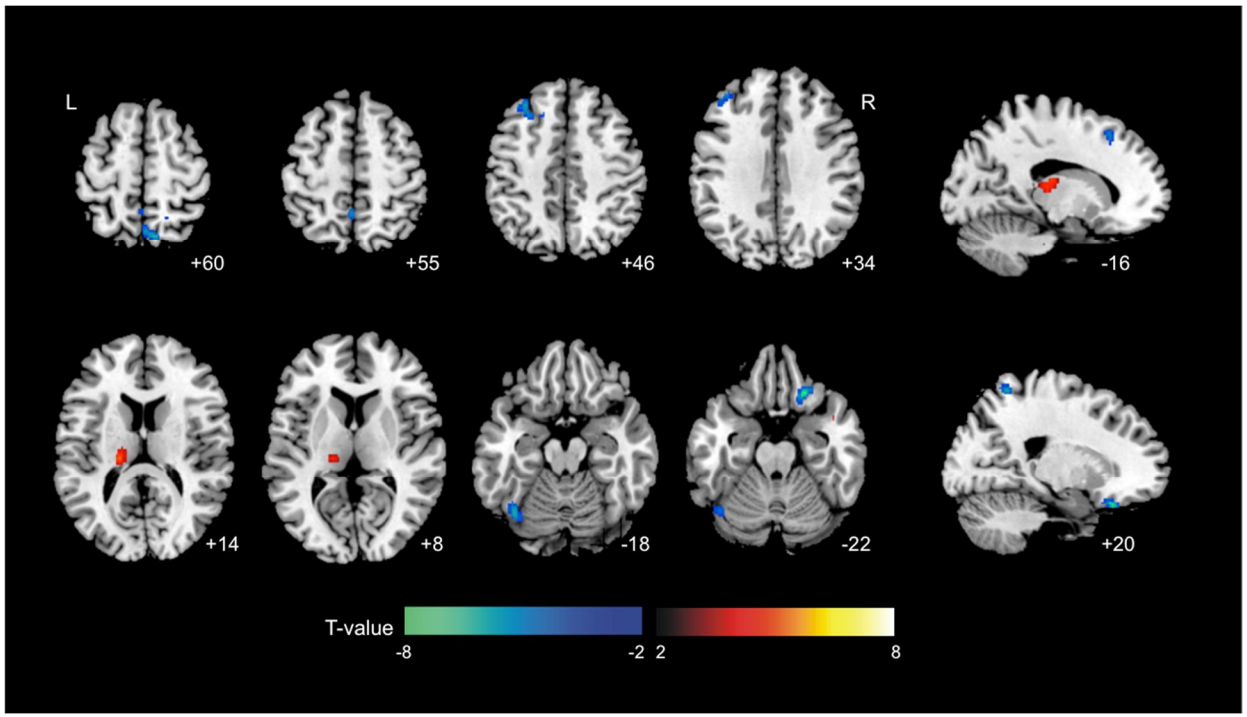

Figure 8. Brain regions showing correlations between observed metabolic changes following transcranial direct current stimulation tDCS and baseline gray matter volume. Significant clusters are overlaid onto an MNI-152 brain template image. The warm color scale indicates a positive correlation and the cool color scale indicates a negative correlation. The labels of each slice indicate the *z*-coordinate for axial slices and the *x*-coordinate for the sagittal slice.L, left; R, right.

Table 8. Brain regions showing correlations between observed metabolic changes following transcranial direct current stimulation tDCS and baseline gray matter volume.

Region	BA	MNI coordinates			t-score	z-score	Cluster size
		x	y	z			
Positive							
L Thalamus		-18	-24	14	5.10	3.31	95
Negative							
R Inferior Frontal Gyrus	47	22	28	-24	10.57	4.54	69
R Precuneus	7	8	-68	60	6.60	3.76	98
L Precuneus	7	-2	-50	56	5.24	3.36	
L Fusiform Gyrus	19	-40	-66	-20	6.52	3.74	121
L Middle Frontal Gryus	8/9	-30	32	46	5.71	3.51	100
L Superior Frontal Gyrus	8/9	-16	24	50	5.34	3.39	
R Superior Parietal Lobule	7	18	-54	64	5.77	3.53	84

L, left; R, Right; BA, brodmann area

3.2.9. Effect of baseline BDI scores on tDCS efficacy and brain metabolic changes

There was no significant correlation between BDI score at baseline and tDCS efficacy in the active tDCS group ($p = 0.181$). However, we found positive metabolic correlations in the left precuneus, right dorsolateral portion of the middle frontal gyrus, and bilateral motor and sensory areas with the BDI baseline score (Figure 9). The bilateral motor and sensory areas included the right premotor (superior frontal gyrus), primary somatosensory area (postcentral gyrus), and left primary and supplementary motor areas (paracentral lobule, medial frontal and precentral gyri). The positive correlation means that patients with a less depressive symptom before treatment showed reduced brain metabolism in those brain regions after tDCS. Brain regions showing negative correlations with BDI scores were the left fusiform and lingual gyrus and the adjacent cerebellum. The negative correlation means that patients with a less depressive symptom before treatment showed increased brain metabolism in those brain regions after tDCS

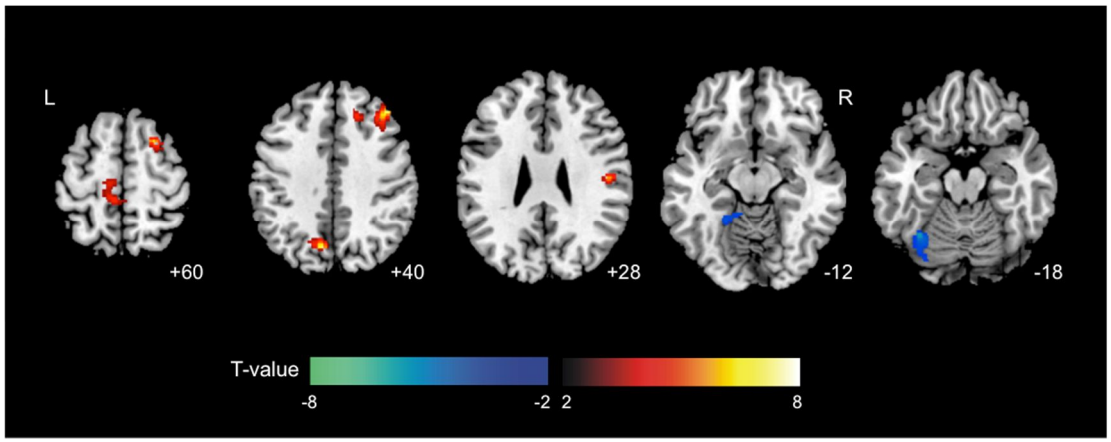

Figure 9. Brain regions showing correlations between observed metabolic changes following transcranial direct current stimulation and scores of Beck Depression Inventroy. Significant clusters are overlaid onto an MNI-152 brain template image. The warm color scale indicates a positive correlation and the cool color scale indicates a negative correlation. The labels of each slice indicate the *z*-coordinate for axial slices. L, left; R, right (98).

3.3. Discussion

3.3.1. tDCS effect on brain regional metabolism: possible mechanisms of tDCS-induced pain relief

To our knowledge, this is the first [^{18}F]FDG-PET imaging study to evaluate the underlying neural mechanisms of tDCS effect on neuropathic pain following SCI. After active tDCS treatment, we found increased metabolism at sites of anodal stimulation, the right caudate and medulla. The left DLPFC showed decreased metabolism after active tDCS, which was negatively correlated with pain relief. Ohn et al (67) also found decreased activity in the DLPFC after rTMS sessions in patients with neuropathic pain after stroke. In this study, patients underwent rTMS sessions on the motor cortex for 5 days and after the stimulations, responders showed decreased activity in the DLPFC by noxious tactile stimulation compared to before rTMS sessions. The DLPFC and brainstem are the key regions of the top-down pain modulatory system (81, 92). In a study of experimentally induced allodynia, brain activation in the DLPFC showed a negative correlation with unpleasantness and perceived pain intensity, supposedly by inhibiting the neuronal coupling in the midbrain–thalamus (79). A recent rTMS study found that the left DLPFC stimulation was associated with reduced pain ratings during allodynia and signal changes in the medulla (81). In addition, it is well described that the prefrontal area is generally related to cognitive and attentional processing of painful stimuli (99, 100). Previous PET studies of patients with neuropathic pain receiving MCS also identified changes in these brain regions. Kishima et al (55) found decreased activity in the DLPFC during the early post-phase (20 minutes after MCS) and suggested that the

reduced activity in the DLPFC might reflect attenuation of attention to and perception of neuropathic pain. Garcia-Larrea et al(52, 56) identified activations in the brainstem during MCS as a part of descending inhibitory processes. From these results, we suggest that the analgesic effects of tDCS are mediated by descending pain modulatory system including DLPFC and medulla.

Although we did not found changes of the precuneus in the analysis for the whole active tDCS patients, significant decreased metabolism in the precuneus was found in the analysis for responders, which also negatively correlated with pain relief. Recently, it has suggested that changes occur in the resting DMN in patients with chronic pain. In patients with chronic back pain, the precuneus showed reduction in deactivation during a simple visual attention task compared with controls (36). Cauda et al(101) found that the DMNs of patients suffering from diabetic pain displayed increased precuneus connectivity compared with those of the healthy controls. Overactivity in DMN is associated with excessive attention to internal state, which may be also associated with hypervigilence to pain and pain-related information that is a main clinical feature seen in many patients with chronic pain (92). These findings suggest that tDCS might contribute to pain relief by normalizing DMN function

3.3.2. Additional brain metabolic changes associated with active tDCS

Metabolic changes in the perigenual ACC (pACC) was showed negative correlations with pain relief. The ACC that is one of the key regions for pain modulation by cognitive and emotional processes (102) was a neurosurgical target for alleviating neuropathic pain (103). Cohen et al(104) found that

patients who underwent cingulotomy for the treatment of intractable pain had impaired attention and behavioral responsiveness. Thus, a focal lesion within the ACC might modulate the affective and attentional process for alleviating pain. From these findings, we could expect that the negative metabolic correlation with pain relief in the pACC may have a similar effect to cingulotomy.

Additionally, the present study found increased metabolism of the left parahippocampus in nonresponders. The increased metabolism in the hippocampal area also found in the analysis of the whole active tDCS patients, but the increase was not significant compared to changes in sham tDCS group. The hippocampus is one of the crucial limbic areas involved in several functions that are impaired in neuropathic pain, such as anxiety, depression, learning, and memory (105, 106). Recent rTMS study for patients with fibromyalgia suggested that the hippocampus is the neural substrate for the improvement of quality of life after rTMS (107). In this study, patients with fibromyalgia underwent rTMS on M1 over 10 weeks and after that, active rTMS group had greater quality of life improvement than the sham stimulation group without effect on pain intensity, and the improvement was associated with a concomitant increased metabolism in the hippocampus. These results suggested that the hippocampal hypermetabolism by rTMS was associated with improvement of the emotional and cognitive dimension of pain rather than a direct effect on the pain perception. From these results, it could be suggested that the hippocampal hypermetabolism in nonresponders found in present study reflects the gap between emotional and cognitive changes and direct improvement of pain ratings after tDCS treatement. For

more detailed mechanisms of hippocampal changes, further studies for changes in emotional and cognitive dimensions are needed.

3.3.3. Effect of baseline gray matter volume on metabolic changes by tDCS

The baseline gray matter volume and metabolic changes in the left thalamus showed positive correlation. The thalamus is one of the main structures that receive projections from multiple ascending pain pathways; therefore, it could be involved in both sensory discriminative and affective-motivational components of pain (27). Previous MCS studies suggested that the thalamus is a necessary step allowing pain relieving by MCS (52). Therefore, the positive correlation between metabolic changes by tDCS and gray matter volume in the left thalamus might suggest that the thalamus is important brain region for effective transmission of cortical excitability made by tDCS to other pain associated brain regions. However, we did not found changes in the thalamus after tDCS. In previous MCS studies, the thalamus activation appeared phasic and short lasting. The activation was reduced 30 min after MCS discontinuation (52), and overall activation during 35-min period of MCS and during 75-min period after discontinuation of MCS did not found thalamus activation (54). These results suggest that the role of the thalamus activation is a trigger for other cortical and subcortical activations. We investigated the changes in brain metabolism the day after end of tDCS session, the changes in thalamus might be averaged out or disappeared.

The negative correlations between metabolic change and the baseline gray matter volume in the precuneus and DLPFC support that these brain regions are important for pain modulation. The decreased metabolism in the

DLPFC and precuneus correlated with the degree of pain relief by tDCS. Moreover, the DLPFC showed decreased metabolism after active tDCS sessions. Relatively normal state of these brain regions could contribute to decreased pain perception through stabilizing of these regions.

3.3.4. Effect of BDI on tDCS efficacy and metabolic changes

The metabolic changes in the left precuneus and right DLPFC after active tDCS showed positive correlation with BDI scores at baseline. This positive correlation means that subjects with less depressive symptom before treatment showed reduced brain metabolism in those brain regions after tDCS. Mood is closely linked to pain perception, and motivation for treatment. Therefore, we cannot rule out the possibility that the changes in the left precuneus and right DLPFC might be associated with depressive symptoms. However, we did not find a significant correlation between tDCS efficacy and BDI scores at baseline, and the BDI scores were not correlated with the brain regions associated with possible mechanisms of tDCS-induced pain relief such as the left DLPFC, medulla, pACC. These findings suggest that the pain relief and brain metabolic changes following tDCS were not confounded by depression.

3.3.5. Effect of tDCS on pain relief

In the present study, patients with neuropathic pain following SCI showed a statistically significant decrease in pain ratings after the active tDCS treatment. However, clinically meaningful improvement was found in only 2 patients (20%) with reductions in pain intensity from baseline of more than 30% and who rated pain as markedly improved (‘much improved’ or ‘very much improved’). The intervention in our study was thus less effective than that in

the study by Fregni et al (64), who found a reduction of 50% or more in the visual analogue scale (VAS) for overall pain in 63% of patients with neuropathic pain following SCI. The reason behind this inconsistency does not appear to be related to the tDCS methodology, because we used essentially the same study protocol as described by Fregni et al (64). Two more recent tDCS studies, also using essentially the same protocol, failed to find any statistically significant reduction in overall pain intensity in patients with neuropathic pain following SCI (108, 109). Wrigley et al (108) suggested that the reason for lack of tDCS efficacy was the long injury duration of their patients (21.3 ± 13.8 years). They mentioned the possibility that central changes resulting from neuropathic SCI pain had become consolidated, so that tDCS could not modulate the central pain-related system. In the present study, however, the injury duration was 2.5 years on average, and was thus shorter than that of the participants in the study by Fregni et al (64). Therefore, we suggest that injury duration was not very likely to contribute to the lack of tDCS efficacy in this study. Soler et al (109), on the other hand, suggested that the analgesic effect of tDCS differed according to the subtype of spontaneous pain. In that study, paroxysmal pain was more reduced than continuous pain, and the pain relief lasted for 12 weeks after treatment. Fregni et al (64) also found that tDCS was more effective for paroxysmal pain than for continuous pain. One of the reasons for the apparently reduced effect of tDCS observed in the present study might be that we considered only overall pain, not the specific type of pain (e.g., paroxysmal or continuous).

Interestingly, all the responders had SCI at cervical level, but most nonresponders had SCI at thoracic level in the present study. I did not find any study investigated association between pain location and efficacy of brain

stimulation. In the previous study of Fregni et al (64) found opposite result from the present study that pain in the lower limbs and thoracic lesion were significantly associated with better outcome compared to pain in the upper limbs/back pain and cervical lesion. However, they did not discuss reason for the result. The result of present study could be coincident because this study had small sample size as well as showed opposite results from the previous study. However, it is possible the effect of tDCS differed by the pain location, so it should be investigated specifically in the future study.

Recent studies demonstrated that tDCS combined with visual illusion reduced pain in SCI patients. The combined intervention led to a greater and more sustained analgesic effect than either intervention alone (109), and pain perception thresholds were increased in patients, who reported reduced ongoing pain after the combined intervention (110). The visual illusion can affect corticospinal excitability, and so it may have a synergistic effect with tDCS. These observations suggest that tDCS combined with other therapeutic approaches may, at least in part, overcome the limitations of indirect stimulation.

3.4. Limitations and suggestions for further studies

This sham-controlled tDCS study was not randomized. Subjects were assigned to the active or sham group according to years of enrollment. Although there were no significant group differences in demographic and clinical characteristic between the active and sham groups, an imbalance of confounding factors might have affected the results. Randomized studies are needed to replicate and refine our findings. Further, brain imaging studies

combining tDCS with sensory stimulation such as pain provocation could provide additional information on the mechanisms of the analgesic effect induced by tDCS (111, 112).

4. General discussion

In this study, we investigated underlying neural mechanisms of neuropathic pain following SCI and of analgesic effect of tDCS. From these studies, first, we identified that the prefrontal area, including the DLPFC and medial frontal cortex, and the precuneus have the important role in disrupted pain modulation in neuropathic pain patients, and second, tDCS on M1 could relieve pain by control of these brain regions. The DLPFC is one of the main regions associated cognitive modulation of pain process. The atrophy in the DLPFC might be associated with excessive attention and awakening to pain and pain-related information that is a main clinical feature of neuropathic pain (92). Moreover, the abnormal DLPFC volume found study 1 showed negative correlation with metabolism in precuneus, one of the brain regions composed of DMN. Overactivity in DMN is associated with excessive attention to internal state, which might be associated with hypervigilance to pain in neuropathic pain patients. In study 2, the DLPFC and precuneus showed decreased metabolism after tDCS treatment, and the stabilizing of two regions correlated with pain relief by tDCS. These results suggest that the increased attention to the pain stimulation and painful state is important reason for chronic pain and tDCS could normalize the increased function. Moreover, the correlation between the DLPFC and precuneus suggest the possibility that the DLPFC modulate DMN.

Based on these results, we expect that tDCS on the DLPFC could be effective treatment strategy to patients with neuropathic pain following tDCS. Brighina et al (113) found significant decreased spontaneous pain induced by capsaicin after rTMS on left DLPFC. Taylor et al. (81) found that the left

DLPFC rTMS was associated with reduced pain ratings during allodynia and signal changes in the medulla. Although these previous studies have suggested that the role of analgesic effect of the DLPFC rTMS, there are lack of studies of the DLPFC stimulation to patients with neuropathic pain. Further study using the DLPFC stimulation to patients with neuropathic pain would contribute to develop of new treatment strategy.

5. Reference

1. Dworkin RH, Backonja M, Rowbotham MC, Allen RR, Argoff CR, Bennett GJ, et al. Advances in neuropathic pain: diagnosis, mechanisms, and treatment recommendations. Arch Neurol. 2003;60(11):1524-34.
2. Nicholson BD. Evaluation and treatment of central pain syndromes. Neurology. 2004;62(5 Suppl 2):S30-6.
3. Woolf CJ, Mannion RJ. Neuropathic pain: aetiology, symptoms, mechanisms, and management. Lancet. 1999;353(9168):1959-64.
4. Finnerup NB, Johannesen IL, Fuglsang-Frederiksen A, Bach FW, Jensen TS. Sensory function in spinal cord injury patients with and without central pain. Brain. 2003;126(Pt 1):57-70.
5. Siddall PJ, McClelland JM, Rutkowski SB, Cousins MJ. A longitudinal study of the prevalence and characteristics of pain in the first 5 years following spinal cord injury. Pain. 2003;103(3):249-57.
6. Widerstrom-Noga E, Biering-Sorensen F, Bryce T, Cardenas DD, Finnerup NB, Jensen MP, et al. The international spinal cord injury pain basic data set. Spinal Cord. 2008;46(12):818-23.
7. Hulsebosch CE, Hains BC, Crown ED, Carlton SM. Mechanisms of chronic central neuropathic pain after spinal cord injury. Brain Res Rev. 2009;60(1):202-13.
8. McAdoo DJ, Xu GY, Robak G, Hughes MG. Changes in amino acid concentrations over time and space around an impact injury and their diffusion through the rat spinal cord. Exp Neurol. 1999;159(2):538-44.
9. Zhang AL, Hao JX, Seiger A, Xu XJ, Wiesenfeld-Hallin Z, Grant G, et al. Decreased GABA immunoreactivity in spinal cord dorsal horn neurons

after transient spinal cord ischemia in the rat. Brain Res. 1994;656(1):187-90.

10. Wiesenfeld-Hallin Z, Aldskogius H, Grant G, Hao JX, Hokfelt T, Xu XJ. Central inhibitory dysfunctions: mechanisms and clinical implications. Behav Brain Sci. 1997;20(3):420-5; discussion 35-513.
11. Christensen MD, Hulsebosch CE. Spinal cord injury and anti-NGF treatment results in changes in CGRP density and distribution in the dorsal horn in the rat. Exp Neurol. 1997;147(2):463-75.
12. Bennett AD, Everhart AW, Hulsebosch CE. Intrathecal administration of an NMDA or a non-NMDA receptor antagonist reduces mechanical but not thermal allodynia in a rodent model of chronic central pain after spinal cord injury. Brain Res. 2000;859(1):72-82.
13. Mills CD, Fullwood SD, Hulsebosch CE. Changes in metabotropic glutamate receptor expression following spinal cord injury. Exp Neurol. 2001;170(2):244-57.
14. Hains BC, Klein JP, Saab CY, Craner MJ, Black JA, Waxman SG. Upregulation of sodium channel Nav1.3 and functional involvement in neuronal hyperexcitability associated with central neuropathic pain after spinal cord injury. J Neurosci. 2003;23(26):8881-92.
15. Drew GM, Siddall PJ, Duggan AW. Responses of spinal neurones to cutaneous and dorsal root stimuli in rats with mechanical allodynia after contusive spinal cord injury. Brain Res. 2001;893(1-2):59-69.
16. Hoheisel U, Scheifer C, Trudrung P, Unger T, Mense S. Pathophysiological activity in rat dorsal horn neurones in segments rostral to a chronic spinal cord injury. Brain Res. 2003;974(1-2):134-45.

17. Hains BC, Waxman SG. Activated microglia contribute to the maintenance of chronic pain after spinal cord injury. J Neurosci. 2006;26(16):4308-17.
18. Saab CY, Hains BC. Remote neuroimmune signaling: a long-range mechanism of nociceptive network plasticity. Trends Neurosci. 2009;32(2):110-7.
19. Zhao P, Waxman SG, Hains BC. Modulation of thalamic nociceptive processing after spinal cord injury through remote activation of thalamic microglia by cysteine cysteine chemokine ligand 21. J Neurosci. 2007;27(33):8893-902.
20. Vallejo R, Tilley DM, Vogel L, Benyamin R. The role of glia and the immune system in the development and maintenance of neuropathic pain. Pain Pract. 2010;10(3):167-84.
21. Treede RD, Kenshalo DR, Gracely RH, Jones AK. The cortical representation of pain. Pain. 1999;79(2-3):105-11.
22. Peyron R, Laurent B, Garcia-Larrea L. Functional imaging of brain responses to pain. A review and meta-analysis. Neurophysiol Clin. 2000;30(5):263-88.
23. Apkarian AV, Bushnell MC, Treede RD, Zubieta JK. Human brain mechanisms of pain perception and regulation in health and disease. Eur J Pain. 2005;9(4):463-84.
24. Seifert F, Maihofner C. Central mechanisms of experimental and chronic neuropathic pain: findings from functional imaging studies. Cell Mol Life Sci. 2009;66(3):375-90.
25. Price DD. Psychological and neural mechanisms of the affective dimension of pain. Science. 2000;288(5472):1769-72.

26. Vogt BA, Sikes RW. The medial pain system, cingulate cortex, and parallel processing of nociceptive information. Prog Brain Res. 2000;122:223-35.
27. Schweinhardt P, Bushnell MC. Pain imaging in health and disease--how far have we come? J Clin Invest. 2010;120(11):3788-97.
28. Iadarola MJ, Max MB, Berman KF, Byas-Smith MG, Coghill RC, Gracely RH, et al. Unilateral decrease in thalamic activity observed with positron emission tomography in patients with chronic neuropathic pain. Pain. 1995;63(1):55-64.
29. Hsieh JC, Belfrage M, Stone-Elander S, Hansson P, Ingvar M. Central representation of chronic ongoing neuropathic pain studied by positron emission tomography. Pain. 1995;63(2):225-36.
30. Egloff N, Sabbioni ME, Salathe C, Wiest R, Juengling FD. Nondermatomal somatosensory deficits in patients with chronic pain disorder: clinical findings and hypometabolic pattern in FDG-PET. Pain. 2009;145(1-2):252-8.
31. Apkarian AV, Sosa Y, Sonty S, Levy RM, Harden RN, Parrish TB, et al. Chronic back pain is associated with decreased prefrontal and thalamic gray matter density. J Neurosci. 2004;24(46):10410-5.
32. Geha PY, Baliki MN, Harden RN, Bauer WR, Parrish TB, Apkarian AV. The brain in chronic CRPS pain: abnormal gray-white matter interactions in emotional and autonomic regions. Neuron. 2008;60(4):570-81.
33. Kuchinad A, Schweinhardt P, Seminowicz DA, Wood PB, Chizh BA, Bushnell MC. Accelerated brain gray matter loss in fibromyalgia patients: premature aging of the brain? J Neurosci. 2007;27(15):4004-7.

34. Sundgren PC, Dong Q, Gomez-Hassan D, Mukherji SK, Maly P, Welsh R. Diffusion tensor imaging of the brain: review of clinical applications. Neuroradiology. 2004;46(5):339-50.

35. Lutz J, Jager L, de Quervain D, Krauseneck T, Padberg F, Wichnalek M, et al. White and gray matter abnormalities in the brain of patients with fibromyalgia: a diffusion-tensor and volumetric imaging study. Arthritis Rheum. 2008;58(12):3960-9.

36. Baliki MN, Geha PY, Apkarian AV, Chialvo DR. Beyond feeling: chronic pain hurts the brain, disrupting the default-mode network dynamics. J Neurosci. 2008;28(6):1398-403.

37. Napadow V, LaCount L, Park K, As-Sanie S, Clauw DJ, Harris RE. Intrinsic brain connectivity in fibromyalgia is associated with chronic pain intensity. Arthritis Rheum. 2010;62(8):2545-55.

38. Shulman GL, Fiez JA, Corbetta M, Buckner RL, Miezin FM, Raichle ME, et al. Common Blood Flow Changes across Visual Tasks: II. Decreases in Cerebral Cortex. J Cogn Neurosci. 1997;9(5):648-63.

39. Raichle ME, MacLeod AM, Snyder AZ, Powers WJ, Gusnard DA, Shulman GL. A default mode of brain function. Proc Natl Acad Sci USA. 2001;98(2):676-82.

40. Fox MD, Raichle ME. Spontaneous fluctuations in brain activity observed with functional magnetic resonance imaging. Nat Rev Neurosci. 2007;8(9):700-11.

41. Kennedy DP, Redcay E, Courchesne E. Failing to deactivate: resting functional abnormalities in autism. Proc Natl Acad Sci USA. 2006;103(21):8275-80.

42. Greicius MD, Flores BH, Menon V, Glover GH, Solvason HB, Kenna H, et al. Resting-state functional connectivity in major depression: abnormally increased contributions from subgenual cingulate cortex and thalamus. Biol Psychiatry. 2007;62(5):429-37.
43. Greicius MD, Srivastava G, Reiss AL, Menon V. Default-mode network activity distinguishes Alzheimer's disease from healthy aging: evidence from functional MRI. Proc Natl Acad Sci USA. 2004;101(13):4637-42.
44. Wrigley PJ, Press SR, Gustin SM, Macefield VG, Gandevia SC, Cousins MJ, et al. Neuropathic pain and primary somatosensory cortex reorganization following spinal cord injury. Pain. 2009;141(1-2):52-9.
45. Gustin SM, Wrigley PJ, Siddall PJ, Henderson LA. Brain anatomy changes associated with persistent neuropathic pain following spinal cord injury. Cereb Cortex. 2010;20(6):1409-19.
46. Tsubokawa T, Katayama Y, Yamamoto T, Hirayama T, Koyama S. Treatment of thalamic pain by chronic motor cortex stimulation. Pacing Clin Electrophysiol. 1991;14(1):131-4.
47. Nguyen JP, Lefaucher JP, Le Guerinel C, Eizenbaum JF, Nakano N, Carpentier A, et al. Motor cortex stimulation in the treatment of central and neuropathic pain. Arch Med Res. 2000;31(3):263-5.
48. Nuti C, Peyron R, Garcia-Larrea L, Brunon J, Laurent B, Sindou M, et al. Motor cortex stimulation for refractory neuropathic pain: four year outcome and predictors of efficacy. Pain. 2005;118(1-2):43-52.
49. Lefaucheur JP, Drouot X, Cunin P, Bruckert R, Lepetit H, Creange A, et al. Motor cortex stimulation for the treatment of refractory peripheral neuropathic pain. Brain. 2009;132(Pt 6):1463-71.

50. Lindblom UF, Ottosson JO. Influence of pyramidal stimulation upon the relay of coarse cutaneous afferents in the dorsal horn. Acta physiolo Scand. 1957;38(3-4):309-18.
51. Andersen P, Eccles JC, Sears TA. Presynaptic inhibitory action of cerebral cortex on the spinal cord. Nature. 1962;194:740-1.
52. Garcia-Larrea L, Peyron R, Mertens P, Gregoire MC, Lavenne F, Le Bars D, et al. Electrical stimulation of motor cortex for pain control: a combined PET-scan and electrophysiological study. Pain. 1999;83(2):259-73.
53. Peyron R, Garcia-Larrea L, Deiber MP, Cinotti L, Convers P, Sindou M, et al. Electrical stimulation of precentral cortical area in the treatment of central pain: electrophysiological and PET study. Pain. 1995;62(3):275-86.
54. Peyron R, Faillenot I, Mertens P, Laurent B, Garcia-Larrea L. Motor cortex stimulation in neuropathic pain. Correlations between analgesic effect and hemodynamic changes in the brain. A PET study. Neuroimage. 2007;34(1):310-21.
55. Kishima H, Saitoh Y, Osaki Y, Nishimura H, Kato A, Hatazawa J, et al. Motor cortex stimulation in patients with deafferentation pain: activation of the posterior insula and thalamus. J Neurosurg. 2007;107(1):43-8.
56. Garcia-Larrea L, Peyron R. Motor cortex stimulation for neuropathic pain: From phenomenology to mechanisms. Neuroimage. 2007;37(Suppl 1):S71-9.
57. Lefaucheur JP, Drouot X, Menard-Lefaucheur I, Zerah F, Bendib B, Cesaro P, et al. Neurogenic pain relief by repetitive transcranial magnetic

cortical stimulation depends on the origin and the site of pain. J Neurol Neurosurg Psychiatry. 2004;75(4):612-6.

58. Khedr EM, Kotb H, Kamel NF, Ahmed MA, Sadek R, Rothwell JC. Longlasting antalgic effects of daily sessions of repetitive transcranial magnetic stimulation in central and peripheral neuropathic pain. J Neurol Neurosurg Psychiatry. 2005;76(6):833-8.
59. Passard A, Attal N, Benadhira R, Brasseur L, Saba G, Sichere P, et al. Effects of unilateral repetitive transcranial magnetic stimulation of the motor cortex on chronic widespread pain in fibromyalgia. Brain. 2007;130(Pt 10):2661-70.
60. Nitsche MA, Paulus W. Excitability changes induced in the human motor cortex by weak transcranial direct current stimulation. J Physiol. 2000;527(Pt 3):633-9.
61. Fregni F, Freedman S, Pascual-Leone A. Recent advances in the treatment of chronic pain with non-invasive brain stimulation techniques. Lancet neurol. 2007;6(2):188-91.
62. Poreisz C, Boros K, Antal A, Paulus W. Safety aspects of transcranial direct current stimulation concerning healthy subjects and patients. Brain Res Bull. 2007;72(4-6):208-14.
63. Boggio PS, Zaghi S, Lopes M, Fregni F. Modulatory effects of anodal transcranial direct current stimulation on perception and pain thresholds in healthy volunteers. Eur J Neurol. 2008;15(10):1124-30.
64. Fregni F, Boggio PS, Lima MC, Ferreira MJ, Wagner T, Rigonatti SP, et al. A sham-controlled, phase II trial of transcranial direct current stimulation for the treatment of central pain in traumatic spinal cord injury. Pain. 2006;122(1-2):197-209.

65. Mori F, Codeca C, Kusayanagi H, Monteleone F, Buttari F, Fiore S, et al. Effects of anodal transcranial direct current stimulation on chronic neuropathic pain in patients with multiple sclerosis. J Pain. 2010;11(5):436-42.

66. Lang N, Siebner HR, Ward NS, Lee L, Nitsche MA, Paulus W, et al. How does transcranial DC stimulation of the primary motor cortex alter regional neuronal activity in the human brain? Eur J Neurosci. 2005;22(2):495-504.

67. Ohn SH, Chang WH, Park CH, Kim ST, Lee JI, Pascual-Leone A, et al. Neural correlates of the antinociceptive effects of repetitive transcranial magnetic stimulation on central pain after stroke. Neurorehabil Neural Repair. 2012;26(4):344-5.

68. Rocher AB, Chapon F, Blaizot X, Baron JC, Chavoix C. Resting-state brain glucose utilization as measured by PET is directly related to regional synaptophysin levels: a study in baboons. Neuroimage. 2003;20(3):1894-8.

69. Maynard FM, Jr, Bracken MB, Creasey G, Ditunno JF, Jr, Donovan WH, Ducker TB, et al. International Standards for Neurological and Functional Classification of Spinal Cord Injury. American Spinal Injury Association. Spinal Cord. 1997;35(5):266-74.

70. Ho PT, Li CF, Ng YK, Tsui SL, Ng KF. Prevalence of and factors associated with psychiatric morbidity in chronic pain patients. J Psychosom Res. 2011;70(6):541-7.

71. Quarantelli M, Berkouk K, Prinster A, Landeau B, Svarer C, Balkay L, et al. Integrated software for the analysis of brain PET/SPECT studies with partial-volume-effect correction. J Nucl Med. 2004;45(2):192-201.

72. Ashburner J, Friston KJ. Voxel-based morphometry--the methods. Neuroimage. 2000;11(6 Pt 1):805-21.

73. Ashburner J. A fast diffeomorphic image registration algorithm. Neuroimage. 2007;38(1):95-113.

74. Calhoun VD, Adali T. Feature-based fusion of medical imaging data. IEEE Trans Inf Technol Biomed. 2009;13(5):711-20.

75. Liu J, Pearlson G, Windemuth A, Ruano G, Perrone-Bizzozero NI, Calhoun V. Combining fMRI and SNP data to investigate connections between brain function and genetics using parallel ICA. Hum Brain Mapp. 2009;30(1):241-55.

76. Li YO, Adali T, Calhoun VD. Estimating the number of independent components for functional magnetic resonance imaging data. Hum Brain Mapp. 2007;28(11):1251-66.

77. Seminowicz DA, Wideman TH, Naso L, Hatami-Khoroushahi Z, Fallatah S, Ware MA, et al. Effective treatment of chronic low back pain in humans reverses abnormal brain anatomy and function. J Neurosci. 2011;31(20):7540-50.

78. Obermann M, Rodriguez-Raecke R, Naegel S, Holle D, Mueller D, Yoon MS, et al. Gray matter volume reduction reflects chronic pain in trigeminal neuralgia. Neuroimage. 2013;74:352-8.

79. Lorenz J, Minoshima S, Casey KL. Keeping pain out of mind: the role of the dorsolateral prefrontal cortex in pain modulation. Brain. 2003;126(Pt 5):1079-91.

80. Krummenacher P, Candia V, Folkers G, Schedlowski M, Schonbachler G. Prefrontal cortex modulates placebo analgesia. Pain. 2010;148(3):368-74.

81. Taylor JJ, Borckardt JJ, Canterberry M, Li X, Hanlon CA, Brown TR, et al. Naloxone-reversible modulation of pain circuitry by left prefrontal rTMS. Neuropsychopharmacology. 2013;38(7):1189-97
82. Miller EK, Cohen JD. An integrative theory of prefrontal cortex function. Annu Rev Neurosci. 2001;24:167-202.
83. Funahashi S. Neuronal mechanisms of executive control by the prefrontal cortex. Neurosci Res. 2001;39(2):147-65.
84. Apkarian AV, Sosa Y, Krauss BR, Thomas PS, Fredrickson BE, Levy RE, et al. Chronic pain patients are impaired on an emotional decision-making task. Pain. 2004;108(1-2):129-36
85. Baliki MN, Petre B, Torbey S, Herrmann KM, Huang L, Schnitzer TJ, et al. Corticostriatal functional connectivity predicts transition to chronic back pain. Nat Neurosci. 2012;15(8):1117-9.
86. Apkarian AV, Baliki MN, Farmer MA. Predicting transition to chronic pain. Curr Opin Neurol. 2013;26(4):360-7.
87. Hawellek DJ, Hipp JF, Lewis CM, Corbetta M, Engel AK. Increased functional connectivity indicates the severity of cognitive impairment in multiple sclerosis. Proc Natl Acad Sci USA. 2011;108(47):19066-71.
88. Whitfield-Gabrieli S, Thermenos HW, Milanovic S, Tsuang MT, Faraone SV, McCarley RW, et al. Hyperactivity and hyperconnectivity of the default network in schizophrenia and in first-degree relatives of persons with schizophrenia. Proc Natl Acad Sci USA. 2009;106(4):1279-84
89. McFadden KL, Cornier MA, Melanson EL, Bechtell JL, Tregellas JR. Effects of exercise on resting-state default mode and salience network activity in overweight/obese adults. Neuroreport. 2013;24(15):866-71.

90. Ohara S, Crone NE, Weiss N, Lenz FA. Attention to a painful cutaneous laser stimulus modulates electrocorticographic event-related desynchronization in humans. Clin Neurophysiol. 2004;115(7):1641-52.
91. Petrovic P, Petersson KM, Ghatan PH, Stone-Elander S, Ingvar M. Pain-related cerebral activation is altered by a distracting cognitive task. Pain. 2000;85(1-2):19-30.
92. Tracey I, Mantyh PW. The cerebral signature for pain perception and its modulation. Neuron. 2007;55(3):377-91.
93. Nitsche MA, Paulus W. Sustained excitability elevations induced by transcranial DC motor cortex stimulation in humans. Neurology. 2001;57(10):1899-901.
94. Fregni F, Boggio PS, Nitsche M, Bermpohl F, Antal A, Feredoes E, et al. Anodal transcranial direct current stimulation of prefrontal cortex enhances working memory. Exp Brain Res. 2005;166(1):23-30.
95. Jensen MP, Turner JA, Romano JM, Fisher LD. Comparative reliability and validity of chronic pain intensity measures. Pain. 1999;83(2):157-62.
96. Farrar JT, Young JP, Jr., LaMoreaux L, Werth JL, Poole RM. Clinical importance of changes in chronic pain intensity measured on an 11-point numerical pain rating scale. Pain. 2001;94(2):149-58.
97. Casanova R, Srikanth R, Baer A, Laurienti PJ, Burdette JH, Hayasaka S, et al. Biological parametric mapping: A statistical toolbox for multimodality brain image analysis. Neuroimage. 2007;34(1):137-43.
98. Yoon EJ, Kim YK, Kim HR, Kim SE, Lee Y, Shin HI. Transcranial direct current stimulation to lessen neuropathic pain after spinal cord injury: A mechanistic PET study. Neurorehabil Neural Repair. 2014;28(3):250-9.

99. Coghill RC, Sang CN, Maisog JM, Iadarola MJ. Pain intensity processing within the human brain: a bilateral, distributed mechanism. J Neurophysiol. 1999;82(4):1934-43.

100. Peyron R, Garcia-Larrea L, Gregoire MC, Costes N, Convers P, Lavenne F, et al. Haemodynamic brain responses to acute pain in humans: sensory and attentional networks. Brain. 1999;122(Pt 9):1765-80.

101. Cauda F, D'Agata F, Sacco K, Duca S, Cocito D, Paolasso I, et al. Altered resting state attentional networks in diabetic neuropathic pain. J Neurol Neurosurg Psychiatry. 2010;81(7):806-11.

102. Vogt BA. Pain and emotion interactions in subregions of the cingulate gyrus. Nature reviews Neuroscience. 2005;6(7):533-44.

103. Wilkinson HA, Davidson KM, Davidson RI. Bilateral anterior cingulotomy for chronic noncancer pain. Neurosurgery. 1999;45(5):1129-36.

104. Cohen RA, Kaplan RF, Moser DJ, Jenkins MA, Wilkinson H. Impairments of attention after cingulotomy. Neurology. 1999;53(4):819-24.

105. Barkus C, McHugh SB, Sprengel R, Seeburg PH, Rawlins JN, Bannerman DM. Hippocampal NMDA receptors and anxiety: at the interface between cognition and emotion. Eur J Pharmacol. 2010;626(1):49-56.

106. Cole J, Costafreda SG, McGuffin P, Fu CH. Hippocampal atrophy in first episode depression: a meta-analysis of magnetic resonance imaging studies. J Affect Disord. 2011;134(1):483-487.

107. Boyer L, Dousset A, Roussel P, Dossetto N, Cammilleri S, Piano V, et al. rTMS in fibromyalgia: A randomized trial evaluating QoL and its brain metabolic substrate. Neurology. 2014;82(14):1231-8.

108. Wrigley PJ, Gustin SM, McIndoe LN, Chakiath RJ, Henderson LA, Siddall PJ. Longstanding neuropathic pain after spinal cord injury is refractory to transcranial direct current stimulation: a randomized controlled trial. Pain. 2013;154(10):2178-84.

109. Soler MD, Kumru H, Pelayo R, Vidal J, Tormos JM, Fregni F, et al. Effectiveness of transcranial direct current stimulation and visual illusion on neuropathic pain in spinal cord injury. Brain. 2010;133(9):2565-77.

110. Kumru H, Soler D, Vidal J, Navarro X, Tormos JM, Pascual-Leone A, et al. The effects of transcranial direct current stimulation with visual illusion in neuropathic pain due to spinal cord injury: an evoked potentials and quantitative thermal testing study. Eur J Pain. 2013;17(1):55-66.

111. Burgmer M, Pogatzki-Zahn E, Gaubitz M, Wessoleck E, Heuft G, Pfleiderer B. Altered brain activity during pain processing in fibromyalgia. Neuroimage. 2009;44(2):502-8.

112. Baliki MN, Geha PY, Fields HL, Apkarian AV. Predicting value of pain and analgesia: nucleus accumbens response to noxious stimuli changes in the presence of chronic pain. Neuron. 2010;66(1):149-60.

113. Brighina F, De Tommaso M, Giglia F, Scalia S, Cosentino G, Puma A, et al. Modulation of pain perception by transcranial magnetic stimulation of left prefrontal cortex. J Headache Pain. 2011;12(2):185-91.

국문초록

신경병증성 통증의 신경학적 기반 및 경두개 직류 전기자극의 진통효과와 관련된 뇌 가소성 연구

윤은진
서울대학교 대학원
의학과 뇌신경과학 전공

신경병증성 통증은 척수손상 환자에게 발생하는 가장 중요한 문제 중 하나로, 다양한 약물 혹은 수술에 의한 치료에도 불구하고 증상이 호전되는 경우는 드물다. 따라서 새로운 치료기법의 개발이 필요하며, 신경병증성 통증의 신경학적 특징을 밝히는 것은 이의 시작이 될 것이다. 특히 뇌의 구조적, 기능적 변화를 통합적으로 이해하는 것이 중요할 것이다. 최근 난치성 신경병증성 통증의 치료를 위한 새로운 치료기법으로 경두개 직류 전기자극이 그 효과를 입증하고 있다. 하지만 정확한 메커니즘은 알려져 있지않아 그 적용에 제한이 있다.

본 연구에서는 16 명의 척수손상 후 신경병증성 손상을 겪는 환자와, 10 명의 정상성인을 대상으로 FDG-PET 과 MRI 검사를 실시하였다. Study 1 에서는 환자의 뇌의 기능적, 구조적 변화를 정상인과 비교하고, 이 차이가 서로 어떠한 상관을 갖는지를 연구하였다. Study 2 에서는 환자를 치료군과 허위자극 군으로 나누어 총 10 일 동안 경두개 직류 자극을 실시 한 후 FDG-PET 영상을 다시 얻어 경두개 직류 자극에 의한 뇌 당대사의 변화를 측정하였다. 또한 치료전의 회백질이 이러한 변화와 갖는 상관을 분석하였다.

Study 1 에서 신경병증성 통증 환자에서 감소된 양쪽 배외측전전두엽의 회백질의 양과, 내측 전전두피질의 감소된 당대사를 발견하였다. 각 영상에서 발견된 차이는 다른 영상의 디폴트 모드 네트워크를 구성하는 쐐기전소엽과 상관을 보였다. Study 2 에서는 경두개 직류 자극 치료군에서 통증 평가가 좋아지는 것을 발견하였다(치료전, 7.6 ± 0.5 ; 치료 후, 5.9 ± 1.8; $z = -2.410$, $p = 0.016$). 연수의 증가된 당대사와 좌측 배외측전전두엽의 감소된 당대사가 치료군에서 허위자극 군과 비교하여 유의하게 발견되었다. 또한, 배외측 전전두엽과 쐐기앞소엽의 변화는 경두개 직류 자극에 의한 통증 완화 정도와 그 영역의 치료전의 회백질의 양과 상관을 보였다.

이상의 결과를 통해, 척수손상 후 신경병증성 통증을 겪는 환자에서 인지적, 정서적 과정을 통한 통증 조절과정이 손상되었으며, 이러한 뇌의 변화가 뇌의 디폴트 모드 네트워크와 상관이 있는 것을

발견하였다. 또한, 경두개 직류 자극에 의한 통증 완화 효과는 이러한 뇌 영역의 조절과 상관을 보였다. 이러한 결과를 바탕으로 추후 통증 조절의 핵심 영역인 배외측 전전두엽을 대상으로 한 경두개 직류 자극의 치료효과를 기대해 볼 수 있다.

주요어: 신경병증성 통증, 척수 손상, 경두개 직류 자극, FDG-양전자방출단층촬영, 자기공명영상, 배외측 전전두엽

학번: 2009-30573